Oncogene (2006) 25, 5994–6002

www.nature.com/onc

ORIGINAL ARTICLE

Identification of expressed genes characterizing long-term survival in malignant glioma patients

R Yamanaka[1], T Arao[2], N Yajima[1], N Tsuchiya[1], J Homma[1], R Tanaka[1], M Sano[1], A Oide[3], M Sekijima[3] and K Nishio[2]

[1]Department of Neurosurgery, Brain Research Institute, Niigata University, Niigata City, Japan; [2]Pharmacology Division, National Cancer Center Research Institute, Chuo-ku, Tokyo, Japan and [3]Mitsubishi Chemical Safety Institute, Ibaraki, Japan

Better understanding of the underlying biology of malignant gliomas is critical for the development of early detection strategies and new therapeutics. This study aimed to define genes associated with survival. We investigated whether genes coupled with a class prediction model could be used to define subgroups of high-grade gliomas in a more objective manner than standard pathology. RNAs from 29 malignant gliomas were analysed using Agilent microarrays. We identified 21 genes whose expression was most strongly and consistently related to patient survival based on univariate proportional hazards models. In six out of 10 genes, changes in gene expression were validated by quantitative real-time PCR. After adjusting for clinical covariates based on a multivariate analysis, we finally obtained a statistical significance level for *DDR1* (discoidin domain receptor family, member 1), *DYRK3* (dual-specificity tyrosine-(Y)-phosphorylation-regulated kinase 3) and *KSP37* (Ksp37 protein). In independent samples, it was confirmed that DDR1 protein expression was also correlated to the prognosis of glioma patients detected by immunohistochemical staining. Furthermore, we analysed the efficacy of the short interfering RNA (siRNA)-mediated inhibition of DDR1 mRNA synthesis in glioma cell lines. Cell proliferation and invasion were significantly suppressed by siRNA against DDR1. Thus, DDR1 can be a novel molecular target of therapy as well as an important predictive marker for survival in patients with glioma. Our method was effective at classifying high-grade gliomas objectively, and provided a more accurate predictor of prognosis than histological grading.
Oncogene (2006) 25, 5994–6002. doi:10.1038/sj.onc.1209585; published online 1 May 2006

Keywords: cDNA array; gene expression profiles; glioma; survival predictor; siRNA

Correspondence: Dr R Yamanaka, Department of Neurosurgery, Brain Research Institute, Niigata University, Asahimachi-dori 1-757, Niigata City 951-8585, Japan.
E-mail: ryaman@bri.niigata-u.ac.jp
Received 7 November 2005; revised 8 March 2006; accepted 8 March 2006; published online 1 May 2006

Introduction

Glioblastoma, which is pathologically the most aggressive form, has a median survival range of only 9–15 months (Karpeh *et al.*, 2001; Stewart, 2002; Stupp *et al.*, 2005). Advances in the basic knowledge of cancer biology and surgical techniques, chemotherapy and radiotherapy have led to little improvement in the survival rates of patients suffering from glioblastoma (Stewart, 2002). Poor prognosis is attributable to difficulties of early detection, and to a high recurrence rate during post-initial treatment observation periods. Therefore, it is important to devise more effective therapeutic approaches, to reveal more clearly the biological features of glioblastoma, and identify novel target molecules for diagnosis and therapy of the disease. Several histological grading schemes exist, but the two-tiered World Health Organization (WHO) system is currently the most widely used (Kleihues and Cavenee, 2000). A high WHO grade correlates with clinical progression and decreased survival. However, there are still many individual variabilities within diagnostic categories, leading to the need for developing additional prognostic markers. As prognostic markers are based on morphology, identification of new treatment strategies is limited. Identification of distinct molecular pathways has become critical for developing molecular targeted therapies.

Recently, developed microarray technology has permitted development of multi-organ cancer classification including gliomas (Ramaswamy *et al.*, 2001; Rickman *et al.*, 2001; Kim *et al.*, 2002; Hunter *et al.*, 2003; Mischel *et al.*, 2004), identification of tumor subclasses (Khan *et al.*, 2001; Mischel *et al.*, 2003; Shai *et al.*, 2003; Sorlie *et al.*, 2003; Liang *et al.*, 2005; Nigro *et al.*, 2005; Wong *et al.*, 2005), discovery of progression markers (Sallinen *et al.*, 2000; Agrawal *et al.*, 2002; van de Boom *et al.*, 2003; Godard *et al.*, 2003; Hoelzinger *et al.*, 2005; Rich *et al.*, 2005; Somasundaram *et al.*, 2005) and prediction of disease outcomes (van't Veer *et al.*, 2002; van de Vijver *et al.*, 2002; Nutt *et al.*, 2003; Freije *et al.*, 2004). Unlike clinicopathological staging, molecular staging can predict long-term outcomes of any individual based on gene expression profile of the tumor at diagnosis. Analysis of expression profiles of genes in

clinical materials is an essential step toward clarifying the detailed mechanisms of oncogenesis and discovering target molecules for the development of novel therapeutic drugs.

The human 1 cDNA microarray (Agilent Technologies, Palo Alto, CA, USA) contains 12 811 clones from more than 7000 UniGene clusters. Each clone is represented by a PCR-amplified, double-stranded complementary DNA (cDNA) product, immobilized on the slide. mRNAs obtained from two biological samples were separately converted to cDNA labeled with distinct fluorescent dyes, usually cyanines 3 (Cy3) and 5 (Cy5), mixed together and hybridized to a single array. Hybridization intensities from the two dyes were measured, and compared for each gene within the array, to identify gene expression differences between the two samples. Utilization of a common reference sample for each array allowed objective comparisons between samples on separate arrays. In the present study, we used agilent cDNA microarrays to define expression patterns to distinguish between short-term and long-term survival of malignant gliomas.

Results

High-grade gliomas in this study

Patients initially showed histologically proven glioblastoma (grade IV), anaplastic astrocytoma or other malignant gliomas (grade III) corresponding to the WHO criteria. Seven patients with grade III and 22 patients with grade IV were included in this study (Table 1). Univariate analysis of clinical features was performed against pathological diagnoses, age, gender and performance status (PS) with respect to survival. Pathological diagnoses, age and gender were not independent predictors of survival (Table 2). Once all gliomas were sorted according to PS, significant difference was found between survival of patients with PS 0–60 and patients with PS 70–100 in our cases (Table 2).

Identification of prognosis-related genes

We performed the univariate proportional hazard model to identify a set of genes that better correlated with censored survival time. Genes were selected if their *P*-value was less than 0.005 and the *P*-value was then used in a multivariate permutation test. We identified 21 genes whose expression was most strongly and consistently related to survival. These genes are listed in Table 3, and include several genes that we believe to be biologically active such as DDR1 (discoidin domain receptor family, member 1) and KSP37 (Ksp37 protein) (see Discussion).

Relationships between results obtained by microarray analysis and by real-time PCR

We chose 10 genes that were not previously associated with gliomas, to measure their mRNA levels by real-time quantitative reverse transcription–PCR. From 29 microarray-measured tumor samples, total RNAs from 27 tumor samples (14 long-term survivors and 13 short-term survivors) were analysed for expressions of ALCAM (activated leukocyte cell adhesion molecule), DDR1, DYRK3 (dual-specificity tyrosine-(Y)-phosphorylation-regulated kinase 3), ITGA5 (integrin alpha 5), ITGB2 (integrin beta 2), KSP37, LDHC (lactate dehydrogenase C), LOC (hypothetical protein

Table 1 Patient characteristics

No.	*Histological diagnosis*	*Age, gender*	*WHO grade*	*PS*	*Survival time*
1	Anaplastic oligoastrocytoma	59, M	III	80	263
2	Anaplastic oligodendroglioma	60, M	III	90	294
3	Anaplastic oligodendroglioma	72, M	III	90	305
4	Anaplastic astrocytoma	32, M	III	100	545
5	Anaplastic astrocytoma	73, M	III	70	617
6	Anaplastic astrocytoma	45, M	III	60	698
7	Anaplastic astrocytoma	65, M	III	90	762
8	Glioblastoma	18, F	IV	60	111
9	Glioblastoma	64, F	IV	50	154
10	Glioblastoma	28, M	IV	70	202
11	Glioblastoma	45, M	IV	60	261
12	Glioblastoma	54, M	IV	40	268
13	Glioblastoma	68, M	IV	80	286
14	Glioblastoma	62, M	IV	70	347
15	Glioblastoma	80, M	IV	80	349
16	Glioblastoma	78, F	IV	60	350
17	Glioblastoma	69, M	IV	90	352
18	Glioblastoma	67, M	IV	50	396
19	Glioblastoma	63, M	IV	60	405
20	Glioblastoma	20, F	IV	90	417
21	Glioblastoma	71, M	IV	80	436
22	Glioblastoma	31, M	IV	90	453
23	Glioblastoma	56, M	IV	80	506
24	Glioblastoma	55, M	IV	80	630
25	Glioblastoma	52, F	IV	90	641
26	Glioblastoma	27, F	IV	90	757
27	Glioblastoma	42, F	IV	70	880
28	Glioblastoma	47, M	IV	90	908
29	Glioblastoma	42, M	IV	90	1189

Abbreviation: PS, performance status; WHO, World Health Organization.

Table 2 Univariate analysis of clinical features

Variable	*No. of patients*	*Median survival time (days)*	P *(log-rank test)*
WHO grade			
Grade III	7	617	0.56
Grade IV	22	417	
Age (years)			
<60	16	641	0.069
⩾60	13	352	
Gender			
Male	22	436	0.979
Female	7	417	
PS			
70–100	21	617	0.0033
0–60	8	309	

Abbreviation: PS, performance status; WHO, World Health Organization.

Table 3 Identification of prognosis-related genes

GenBank	*Symbol*	*Description*	*Hazard ratio*	P-*value*
BC005261	SLN	Sarcolipin	0.41	0.000263
U13680	LDHC	Lactate dehydrogenase-C	0.24	0.000851
AL1 37662	NRBP2	Nuclear receptor binding protein 2	5.5	0.00101
AB021123	KSP37	Ksp37 protein	0.12	0.00102
M20681	GLUT3	Glucose transporter-like protein-III	0.37	0.00107
BC007952	PKM2	Pyruvate kinase, muscle	0.15	0.0013
N92498	PDCD4	Programmed cell death 4	3.1	0.00205
M10036	TPI1	Triosephosphate isomerase 1	0.16	0.00222
BC015061	RAB32	RAB32, member RAS oncogene family	0.51	0.00260
U20362	TTC10	Intraflagellar transport 88 homolog	4.5	0.00290
BE045190	DDR1	Discoidin domain receptor family, member 1	4.2	0.00308
AF327561	DYRK3	Dual-specificity tyrosine-(Y)-phosphorylation regulated kinase 5	0.17	0.00312
BC005861	ITGB2	Integrin, beta 2	4.1	0.00352
BAB22510		Putative	8.0	0.00365
BC007835	STK40	Serine/threonine kinase 40	0.40	0.00369
AB026706	EMILIN2	Elastin microfibril interfacer 2	0.27	0.00389
AF231512	RBM8B	RNA binding motif protein 8B	4.3	0.00403
BC008786	ITGA5	Integrin, alpha 5	0.36	0.00419
AA404652	ISGF3G	Interferon-stimulated transcription factor 3, gamma (48 kD)	2.8	0.00431
Y10183	ALCAM	Activated leukocyte cell adhesion molecule	2.8	0.00440
MI 9482	ATP synthase	Human ATP synthase beta subunit gene, exons 1–7	0.28	0.00445

A subset of the 21 genes expressed differentially in good and poor prognosis group, listed by category. Included with name of each gene is the GeneBank accession number, a brief description of the gene and the *P*-value that was computed.

Table 4 mRNA levels by real-time quantitative RT–PCR

	Short-term survivor (n=13)	*Long-term survivor (n=14)*	P
ALCAM (ng/ml)	6.6±14.5	0.06±0.1	<0.05
DDR1 (pg/ml)	416.8±56.5	40.6±11.1	<0.01
DYRK3 (ng/ml)	116.1±96.2	449.3±108.7	<0.05
ITGA5 (pg/ml)	38.7±47.1	707.6±85.6	<0.01
ITGB2 (pg/ml)	0.02±0.01	0.03±0.05	NS
KSP37 (pg/ml)	18.9±24.6	8402.9±855.6	<0.01
LDHC (pg/ml)	1.4±1.0	7.5±12.5	NS
LOC (pg/ml)	1.2±1.1	1.7±2.1	NS
SLN (pg/ml)	8.9±1.9	15.5±4.5	<0.05
SLC2A3 (ng/ml)	7.5±8.3	19.1±23.9	NS

Abbreviations: NS, not significant; RT-PCR, reverse transcription–PCR. For other abbreviations, see Table 3.

Table 5 Multivariate analysis

Variable	*Hazard ratio*	*95% CI*	P
WHO grade	9.55	1.24–73.8	0.0305
Age (≥60)	5.88	1.1–31.4	0.038
Gender (male)	8.16	0.748–88.9	0.0851
PS (70–100)	18.2	2.47–134	0.0044
DDR1	21.5	2.12–217	0.0094
DYRK3	0.067	0.006–0.798	0.0325
KSP37	0.008	0.000–0.235	0.0053
ITGA5	0.698	0.146–3.34	0.6525
SLN	2.85	0.658–12.4	0.1615
ALCAM	1.67	0.446–6.274	0.4453

Abbreviations: CI, confidence interval; PS, performance status; WHO, World Health Organization. For other abbreviations see Table 3.

LOC340371), SLN (sarcolipin) and SLC2A3 (solute carrier family 2 member 3). Results are shown in Table 4, and are expressed as means±standard deviation (s.d.). Patterns of gene expression between long- and short-term survivors analysed by microarray paralleled patterns observed using real-time PCR for ALCAM, DDR1, DYRK3, ITGA5, KSP37 and SLN (Table 3).

DDR1, DYRK3 and KSP37 were selected based on a multivariate analysis

To adjust for relevant clinical covariates against six PCR-confirmed genes, we performed a multivariate analysis (Table 5). In incorporating multivariate analysis, high DDR1 expression was negatively correlated with survival ($P=0.0094$; hazard ratio = 21.5; 95% confidence interval (CI), 2.12–217), high DYRK3 expression was positively correlated with survival ($P=0.0325$; hazard ratio = 0.067; 95% CI, 0.006–0.798) and high KSP37 expression was positively correlated with survival ($P=0.0053$; hazard ratio = 0.008; 95% CI, 0.000–0.235). The expression of DDR1 and KSP37 were more closely correlated with survival compared to histological grade (Table 5). Thus, in gliomas, these results suggested that expression of *DDR1*, *DYRK3* and *KSP37* might be a strong predictive factor for patient's survival better than WHO grading.

Immunohistochemical analysis of potential candidate genes

To confirm our results from microarray analysis, we chose to investigate DDR1 expression as a prognostic marker for glioma and performed the immunohistochemical analysis. Firstly, we analysed the protein expression of DDR1 against 29 microarray-measured specimens, and investigated the correlations with patient survivals. DDR1 was expressed in the cytoplasm of neoplastic cells and patients were divided into two

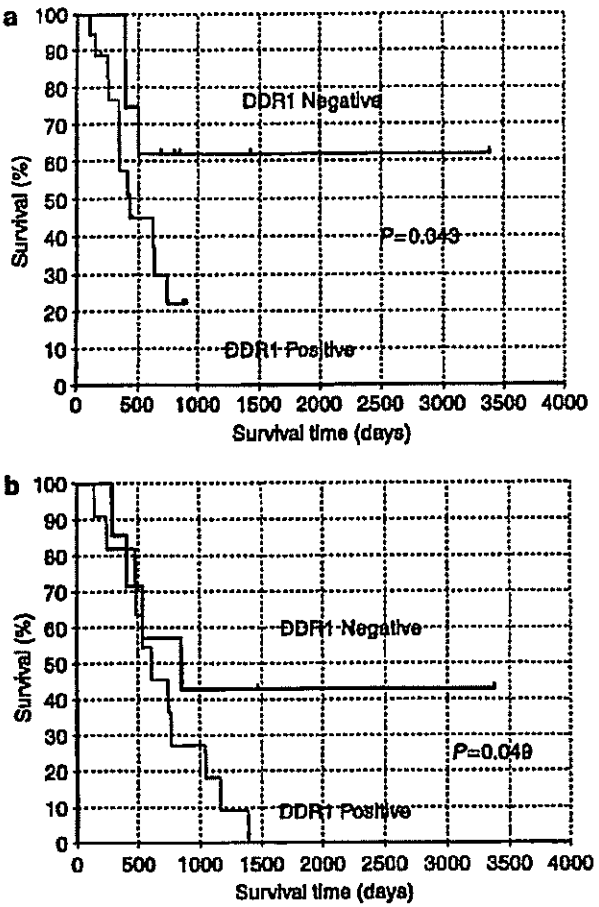

Figure 1 DDR1 protein expressions and patient survivals. Kaplan–Meier survival curves for patients, stratified according to levels of DDR1 expressions in tumors (low DDR1 staining: 0–1 score; high DDR1 staining: 2–3 score; log-rank test). (a) A significant trend for worse outcome was observed in the DDR1-positive group ($P=0.043$). (b) DDR1 protein expressions and patient survivals in independent groups of gliomas. Kaplan–Meier survival curves for patients, stratified according to levels of DDR1 expressions in tumors (low DDR1 staining: 0–1 score; high DDR1 staining: 2–3 score; log-rank test). A significant trend for worse outcome was observed in the DDR1-positive group ($P=0.049$).

groups: positive and negative groups according to immunostaining score. Positive staining for DDR1 was confirmed to be associated with unfavorable overall survival time ($P=0.043$; Figure 1a). Next, in new independent 19 glioma samples, similar results were obtained ($P=0.049$; Figure 1b). Although our results were based on relatively small sample size, the correlation between DDR expression and survival was confirmed by real-time quantitative PCR and also confirmed immunohistochemical analysis in independent samples.

Glioma cell proliferation and invasion are inhibited by DDR1 siRNA

DDR1 overexpression was linked to aggressiveness of glioma in our analysis. In order to determine whether downregulation of endogenous DDR1 suppresses proliferation and invasive behavior of gliomas, we synthesized short interfering RNA (siRNAs) against DDR1 mRNA to reduce expression of DDR1 protein. We analysed efficacy of siRNA-mediated inhibition of DDR1 mRNA synthesis in U251, GI-1, and T98G cells by real-time PCR. As shown in Figure 2a, when U251 cells were transfected with siRNAs against DDR-1 (DDR1-#1 and DDR1-#2), DDR1 mRNA was downregulated 48 h later ($P<0.01$), whereas transfection with a related control siRNA failed to modify DDR1 mRNA expression. When GI-1 and T98G cells were transfected with siRNAs against DDR-1 (DDR1-#1 and DDR1-#2), DDR1 mRNA was downregulated by 10–15% of control siRNA ($P<0.01$).

After transfection with siRNAs against DDR-1, U251 cell counts within 48 h were approximately 40–60% of untreated or control-siRNA-treated cells during this same period of time ($P<0.01$; Figure 2b). GI-1 and T98G cell counts within 48 h were approximately 35–50% of untreated or control-siRNA-treated cells during this same period of time ($P<0.01$). Cell proliferation was significantly suppressed by siRNA against DDR1, as reflected in reduction of mRNA expression.

For invasion assays, transfectants were seeded onto Matrigel-coated invasion chambers, incubated for 24 h and total numbers of cells on the underside of each filter were determined. As shown in Figure 2c, transfections of U251 cells with anti-DDR1 siRNA inhibited cell invasion through the Matrigel by more than 80%, whereas the use of control siRNA had no effect ($P<0.01$). Transfections of GI-1 and T98G cells with anti-DDR1 siRNA inhibited cell invasion through the Matrigel by more than 70–80%, whereas the use of control siRNA had no effect ($P<0.01$). Therefore, invasion by cells was significantly suppressed by siRNA against DDR1, as reflected by reduced mRNA expression.

Discussion

Several works (Sallinen *et al*., 2000; Khan *et al*., 2001; Ramaswamy *et al*., 2001; Rickman *et al*., 2001; Agrawal *et al*., 2002; Kim *et al*., 2002; Veer *et al*., 2002; Vijver *et al*., 2002; Boom *et al*., 2003; Godard *et al*., 2003; Hunter *et al*., 2003; Mischel *et al*., 2003; Nutt *et al*., 2003; Shai *et al*., 2003; Sorlie *et al*., 2003; Freije *et al*., 2004; Mischel *et al*., 2004; Hoelzinger *et al*., 2005; Liang *et al*., 2005; Nigro *et al*., 2005; Rich *et al*., 2005; Somasundaram *et al*, 2005; Wong *et al*., 2005) showed the usefulness of utilizing methods of analysis of multiple forms of data including both clinical and multiple genes, to achieve a more precise discrimination of outcomes for individual patients. The same logical use of multiple forms of data and methods of analysis has been applied in the present study to accurately achieve better classification and prediction of glioma patients. In the present study, we used expression arrays to identify genes that reflect patient's survival. The groups of patients used represented the two extremes of

glioma with respect to outcomes. Nutt *et al.* (2003) and Freije *et al.* (2004) reported the use of microarrays to predict outcomes for glioma patient. Nutt *et al.* involved a group of 50 glioma patients who were not selected based on survival duration. The investigators used Affymetrix U 95 GeneChips to develop a model to classify cases into unfavorable and favorable groups that exhibited significantly different survivals. They picked up 20 genes different from our study that highly correlated with class distinction. On the other hand, Freije *et al.* (2004) also reported the use of microarrays to predict outcomes for all histological types of 85 gliomas. The investigators used Affymetrix HG 133 GeneChips to develop a 44-gene model to classify cases into unfavorable and favorable groups that exhibited significantly different survivals. From these two studies, there were no attempt to predict survivals of individual patients, but results were consistent with ours, and together suggested that clinical differences in outcomes were reflected in global patterns of gene expression that could be appreciated using microarrays.

Some of the genes that were critical components of patterns that were used to discriminate between long-term and short-term survivors are known to affect virulence of the malignant phenotype. Several groups have confirmed prognostic markers of glioma such as Insulin-like growth factor-binding protein 2 (IGFBP2) (Kim *et al.*, 2002; Godard *et al.*, 2003), vascular endothelial growrh factor (VEGF) (Godard *et al.*, 2003), Osteonectin, Doublecortex, Semaphorin 3B (Rich *et al.*, 2005) and brain-type fatty acid-binding protein (FABP7) (Liang *et al.*, 2005).

We have selected *DDR1*, *KSP37* and *DYRK3* from a 21-gene model (21 genes derived from multivariate analysis) to classify cases into unfavorable and favorable groups that exhibited significantly different survivals. We observed that glioma cell proliferation and invasion were significantly suppressed by siRNA against DDR1. The DDR1 is a tyrosine receptor kinase activated by various types of collagen, and is involved in cell–matrix communication (Vogel, 1999). DDR1 is activated independently of β1 integrin (Vogel *et al.*, 2000). DDR1–collagen interaction facilitates the adhesion, migration, differentiation/maturation and cytokine/chemokine production of leukocytes (Yoshimura *et al.*, 2005). DDR1 is overexpressed in several tumors including high-grade brain, esophageal and breast cancers (Weiner and Zagzag, 2000). Based on our data and Ram *et al.* (2005), DDR1 may play a potential role in proliferation and invasion of gliomas. Invasive phenotype is caused by activation of matrix metalloproteinase-2 in DDR1-overexpressing cells (Ram *et al.*, 2006). Glioma cell adhesion, including intercellular and

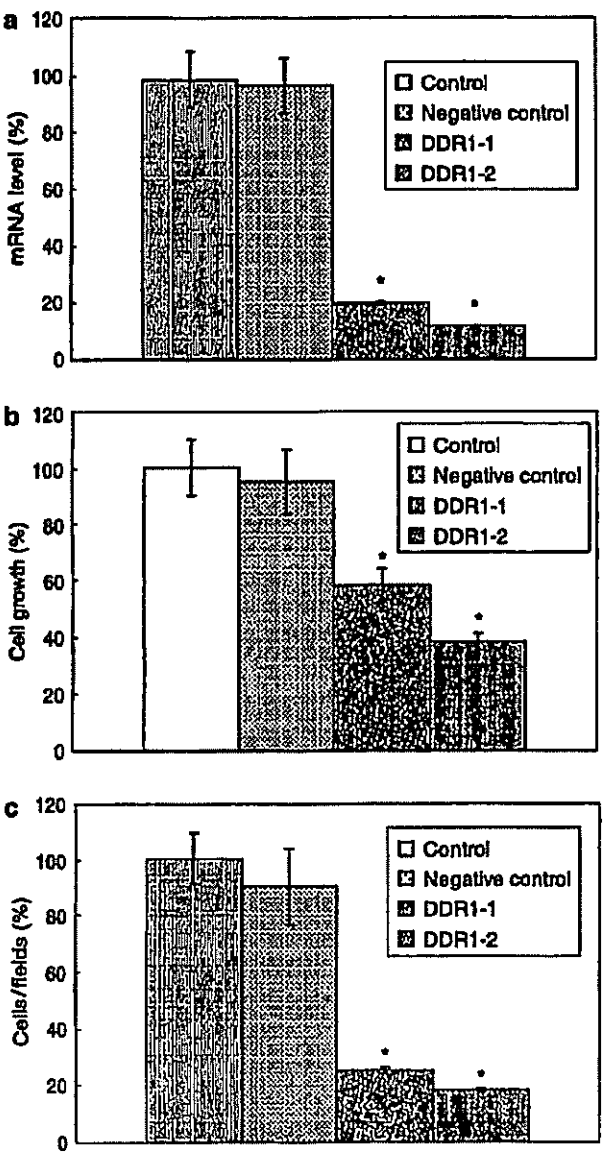

Figure 2 Effects of DDR1 knockdown by RNA interference on proliferation and invasiveness of human glioma cell lines. U251 cells were transiently transfected with short interfering RNAs (siRNA) and subjected to semiquantitative PCR analysis, proliferation assay or Matrigel invasion assays. (a) Reduction of DDR1 mRNA expression by siRNAs against DDR1 was determined by semiquantitative PCR analysis. Transfection with DDR1 siRNAs significantly reduced DDR1, whereas transfection with siRNAs targeted to an unrelated mRNA had no effect on DDR1 expression. $^{*}P<0.01$ compared with both control groups. (b) Cell proliferation assay. Cells were cultured in 96-well plates in 100 μl of serum-enriched medium. When 80% confluence was reached, 25 μl of 100 nM siRNA in cytofectin was added drop wise. Numbers of viable cells were evaluated after 48 h culture by incubation with Tetra color one, and numbers obtained were compared with those of controls. After transfection with DDR1 siRNAs, U251 cell counts within 48 h were approximately 40–60% of untreated or control-siRNA-treated cells during this same period of time. $^{*}P<0.01$ compared with both control groups. (c) For the invasion assays, transfectants were seeded onto Matrigel-coated invasion chambers and incubated for 24 h. Total numbers of cells on the underside of each filter were determined. Invading cells were significantly suppressed by siRNAs against DDR1, as reflected by reduction of mRNA expression. Control, no siRNA treatment; negative control, control siRNA treated. DDR1-#1, DDR1-#2; DDR1 siRNA treated. $^{**}P<0.01$ compared with both control groups.

cell–matrix adhesions, is critical to the maintenance of structural integrity, polarity and cell–cell communication, and their expression is frequently observed in tumor cells concordant with a breakdown of cellular organization, causing an uncontrolled leakage of nutrients and other factors necessary for the survival and growth of tumor cells, and loss of cell–cell contact inhibition leading to increased cell motility. Thus, DDR1 may be a novel molecular target for therapy, and provide an important predictive marker for survival in patients with glioma. KSP37 protein is constitutively secreted by Th1-type CD4-positive lymphocytes and lymphocytes with cytotoxic potential, and may be involved in an essential process of cytotoxic lymphocyte-mediated immunity (Ogawa *et al*., 2001). Down-regulation of KSP37 protein may correlate with poor prognosis of glioma patients with immunosuppressive state. DYRK3 is a member of dual-specificity tyrosine-regulated kinases with roles in cell growth and development. DYRK3 was reported to be expressed in erythroid progenitor cells, and to play roles in kinase activation (Li *et al*., 2002). Although KSP37 and DYRK3 are unique molecules, their roles in glioma progression are unclear, and should be further investigated in the future.

Regardless of their roles in tumorigenesis, all these markers offer potential clinical applications for the treatment and detection of malignant gliomas. To our knowledge, this study is the first to address these molecules as molecular targets for therapeutics. Values of gene-expression-based predictors for prognosis of malignant glioma patients will not be fully realized until additional therapies are available for patients destined to have poor survival, following conventional chemotherapy. In this regard, expression profiles may not only predict the likelihood of long-term survival following nitrosourea chemotherapy, but may also yield clues on individual genes involved in tumor development, progression and response to therapy. It is likely that some of the most differentially expressed genes such as those discussed above will represent therapeutic molecular targets. Moreover, the ability to histologically distinguish ambiguous gliomas will enable appropriate therapies to be tailored to specific tumor subtypes. Class prediction models based on defined molecular profiles allow classification of malignant gliomas in a manner that will better correlate with clinical outcomes than with standard pathology.

Materials and methods

Patients

Mean age of patients was 53.2 years old (range, 18–80). Twenty-two patients were men and seven were women. Tissues were snap-frozen in liquid nitrogen within 5 min of harvesting, and stored thereafter at −80°C. Clinical stage was estimated from accompanying surgical pathology and clinical reports. Samples were specifically re-reviewed by a board-certified pathologist in our institution, using observation of sections of paraffin-embedded tissues that were adjacent or in close proximity to the frozen sample from which the RNA was extracted. Histopathology of each collected specimen was reviewed to confirm adequacy of the sample (i.e., minimal contamination with non-neoplastic elements), and to assess the extent of tumoral necrosis and cellularity. Histological characteristics of tumor samples and clinical disease stage were included as supplements in Table 1.

After surgical resection of tumor, patients had a course of external beam radiation therapy (standard dose of 40 Gy to the tumor with a 3-cm margin, and 20 Gy boost to the whole brain) and nitrosourea-based chemotherapy. Patients were monitored for recurrences of tumor during the initial and maintenance therapy by magnetic resonance imaging or computed tomography. Treatments were carried out at the Department of Neurosurgery, Niigata University Hospital. Informed consent was obtained from all patients for the use of samples in accordance with the guidelines of the Ethical Committee on Human Research, Niigata University Medical School. Overall survival was measured from the date of diagnosis. Survival end points corresponded to dates of death or last follow-up.

RNA extraction

Total RNA was extracted with 1 ml Isogen (Nippongene, Toyama, Japan) per 100 mg frozen glioma tissues, following the manufacturer's instructions. Each tissue type was homogenized with a Polytron (Fisher Scientific) for 30 s and cleared by a 10-min centrifugation at 10 000 *g*. For each ml Isogen, 0.2 ml chloroform was added and samples were vigorously shaken for 20 s and then incubated on ice for 10 min. The aqueous phase was separated by centrifugation at 10 000 *g* for 10 min, decanted and an equal volume of isopropanol was added. The mixture was allowed to precipitate for 10 min and the precipitate was collected by centrifugation at 12 000 *g* for 10 min. The pellet was washed with 70% ethanol, collected by brief centrifugation, air dried and re-suspended in H_2O. RNA was further purified using an RNeasy column (Qiagen, Valencia, CA, USA). The purified RNA was quantified using a UV spectrophotometer, and RNA quality was evaluated by capillary electrophoresis on an Agilent 2100 Bioanalyzer (Agilent Technologies). Only samples with 28S/18S ratios >0.7 and with no evidence of ribosomal peak degradation were included in the study.

Agilent cDNA microarrays

Agilent human 1 cDNA microarrays (Agilent Technologies) contained 13 156 clones from Incyte's human cDNA library. Test and normal brain RNAs were labeled with both Cy3-dCTP and Cy5-dCTP nucleotides (Amersham Biosciences, Tokyo, Japan) and hybridized on two slides (dye-swap hybridizations) according to the direct-labeling method provided by the manufacturer. Following hybridization, slides were scanned and analysed using the Feature Extraction software (version A.4.0.45, Agilent Technologies), as recommended by the manufacturer. Spots that did not pass quality control procedures in the Feature Extraction software were flagged and removed from further analysis. Clones with the same GenBank accession number were averaged.

Expression profiling on Agilent cDNA microarrays

Total RNA (20 μg) was reverse transcribed using the Agilent direct-label cDNA synthesis kit (Agilent Technologies), following the manufacturer's directions. Labeled cDNA was purified using QIAquick PCR Purification columns (Qiagen, Valencia, CA, USA), followed by concentration by vacuum centrifugation. cDNA was suspended in hybridization buffer and hybridized to Agilent human 1 cDNA microarrays (Agilent Technologies) for 17 h at 65°C, according to the

Agilent protocol. To avoid generation of false between-group differences by randomly pairing glioma samples on the two-channel cDNA arrays, each sample was individually labeled and co-hybridized with a normal brain sample labeled with a complementary dye. Normal brain samples were generated by pooling equal amounts of RNA from each control sample and labeling as for individual samples. In addition, Cy dye switch hybridizations were performed for each sample. Normal brain samples were purchased from Clontech (Tokyo, Japan). All microarray data and clinical features have been submitted to Gene Expression Omnibus (GEO, http://www.ncbi.nlm.nih.gov/geo; accession no. GSE4381).

Statistical analysis

Univariate analysis for clinical features was performed by log-rank test using SAS software ver. 9.1.3 (SAS Institute Inc., Cary, NC, USA). In microarray analysis, normalization and survival analysis were performed using the BRB Array Tools software ver. 3.3.0 (http://linus.nci.nih.gov/BRB-ArrayTools.html) developed by Dr Richard Simon and Amy Peng. In brief, a log base 2 transformation was applied to the microarray raw data, and global normalization was used to median the center of log ratios on each array in order to adjust for differences in labeling intensities of the Cy3 and Cy5 dyes. Genes showing minimal variation across the set of arrays were excluded from the analysis. Genes whose expression differed by at least 1.5-fold from the median in at least 20% of the arrays were retained. Genes were also excluded if percent of data missing or filtered out exceeds 50%. Then, genes that passed filtering criteria were considered for further analysis.

We computed a statistical significance level for each gene based on univariate proportional hazards models ($P<0.005$) and identified genes whose expression was significantly related to survival of the patient. These P-values were then used in a multivariate permutation test in which survival times and censoring indicators were randomly permuted among arrays. To adjust the expression of six candidate genes (DDR1, DYRK3, KSP37, ITGA5, SLN and ALCAM) for clinical features (WHO grade, age, gender, PS), clinical data and normalized microarray expression data of six genes were imported into SAS software ver. 9.1.3 (SAS Institute Inc.) and Cox regression model was performed for multivariate analysis against each variable (WHO grade, age, gender, PS, expression levels of six genes). Three samples were excluded for multivariate analysis because there were a few defected expression data. A P-value <0.05 was considered significant. The differences between subgroups of DDR1 siRNA and control groups were tested for statistical significance using the analysis of variance test and statistical significance was determined at the $P<0.01$ level.

Validation of differential expression by real-time quantitative PCR

Total RNA (2 μg) was subjected to DNase treatment in a 10 μl reaction containing 1 μl 10 × DNase I reaction buffer (Invitrogen, Tokyo, Japan) and 1 μg DNase I at room temperature for 10 min. Ethylenediamine tetraacetic acid (1 μl, 25 mM) and 1 μl oligo dT (0.5 μg/μl; Invitrogen) were added to the DNase reaction, and heated to 70°C for 15 min to inactivate DNase I activity and eliminate RNA secondary structure. Samples were placed on ice for 2 min and collected by brief centrifugation. RNA was then reverse-transcribed into cDNA by adding 8 μl master mix containing 4 μl of 5 × first strand buffer, 2 μl dithiothreitol (0.1 M), 1 μl dNTPs (10 mM each) and 1 μl SuperScript II (200 U/μl) (Invitrogen), followed by incubation at 42°C for 45 min. The reaction was diluted 10-fold with dH_2O and stored at 4°C.

Each sample was subjected to 40 cycles of real-time PCR with a LightCycler (Idaho Technology, Salt Lake City, UT, USA). PCR reagents contained 1 × LightCycler DNA Master SYBR Green I (Roche Molecular Biochemicals, Mannheim, Germany), 0.5 μM of each primer, 3 mM $MgCl_2$ and 2 μl cDNA template. PCR conditions were as follows: one cycle of denaturing at 95°C for 10 min, followed by 40 cycles of 95°C for 15 s, 55°C for 5 s and 72°C for 10 s. A melting curve was obtained at the end of amplification cycles to verify specificity of the PCR products. Points at which signal fluorescence exceeded background, for each sample and for each gene, were compared to a standard curve generated by four, 10-fold serial dilutions of concentrated cDNA control of each sample subjected to real-time analysis to determine an expression value. All determinations were performed in duplicate. A Student's t-test was conducted to analyse expression values for long- and short-term survivors to determine statistical significance. For amplification of target genes, the following primers were used (Takara, Yotsukaichi, Japan):

ALCAM-FW:	5′-CCAGATGGCAATATCACATGGTACA-3′,
ALCAM-RW:	5′TCCAGGGTGGAAGTCATGGTATAGA-3′,
DDR1–FW:	5′ACTTTGGCATGAGCCGGAAC-3′,
DDR1–RW:	5′ACGTCACTCGCAGTCGTGAAC-3′,
DYRK3-FW:	5′AGCTGCCTCCAGTTGTTGGGAATAG-3′,
DYRK3-RW:	5′TGCATCTCTGGGCATATCTCTGTC-3′,
ITGA5-FW:	5′TCCCAGTAAGCGACTGGCATC-3′,
ITGA5-RW:	5′GTTCCAGCACACCCTGGCTAA-3′,
ITGB2-FW:	5′ATCGTGCTGATCGGCATTCTC-3′,
ITGB2-RW:	5′GGTTCATGACCGTCGTGGTG-3′,
KSP37-FW:	5′CTTCCGAGGGTGACAGGTGA-3′,
KSP37-RW:	5′TCCAGTGTGAGAACGTTGGATTG-3′,
LDHC-FW:	5′TCATCTGTACTGATTGCGCCAAG-3′,
LDHC-RW:	5′ACGGCACCAGTTCCAACAATAGTAA-3′,
LOC340371-FW:	5′GGAACATGCCAGGGCTTCA-3′,
LOC340371-RW:	5′CTGCTCAACACGGTCTGGA-3′,
SLN-FW:	5′GGAGTTGGAGCTCAAGTTGGAGAC-3′,
SLN-RW:	5′GAACTGCAGGCAGATTTCTGAGG-3′,
SLC2A3-FW:	5′GCCTTTGGCACTCTCAACCAG-3′,
SLC2A3-RW:	5′GCTGCACTTTGTAGGATAGCAGGAA-3′.

Immunohistochemistry

Sections (5 μm) from formalin-fixed, paraffin-embedded tissue specimens were deparaffinized in xylene and dehydrated in a graded series of ethanol, followed by a phosphate-buffered saline (PBS) wash. Antigen retrieval was carried out by incubation at 121°C for 10 min in 10 mM sodium citrate (pH 6.0), followed by incubation with 0.3% H_2O_2 to quench endogenous peroxidase activity. Slides were blocked in 10% normal serum and incubated with rabbit polyclonal anti-DDR1 antibody (dilution 1:50; Santa Cruz Biotechnology, Santa Cruz, CA, USA) for 16 h at 4°C. After washing, the slides were incubated with an avidin–biotin–peroxidase system (Vectastain elite ABC kit, Vector Labs, Burlingame, CA,

USA). Finally, sections were exposed for 10–20 min to 0.01% 3,3-diaminobenzidine (Sigma, Tokyo, Japan) and PBS containing 0.01% hydrogen peroxide. Immunohistochemistry scoring was performed as follows. Staining intensity was classified as none (0 point), weak (1 point), moderate (2 point) or strong (3 point). Intensity of signal of stained areas was estimated by light microscopy, based on 25 percentiles in a representative field. Scores were calculated as weighted averages (sum of points × area%). Averages of three independent measurements were calculated to the first decimal place and used for statistical analysis. Observers were not aware of case numbers.

siRNA treatment and cell proliferation assay

Specific siRNA oligonucleotides directed against human DDR1 were purchased from Invitrogen. The Validated Stealth sequence information is DDR1-#1: 5′-GCUAUGUGGAGAU GGAGUUUGAGUU-3′ and DDR1-#2: 5′-GGCCCUGG UUACUCUUCAGCGAAAU-3′. siRNAs were introduced into glioma cell lines by cytofectin-mediated transfection according to the manufacturer's instructions (Qiagen, Tokyo, Japan). Cells were cultured in 96-well plates in 100 μl of serum-enriched medium. When 80% confluence was reached, 25 μl 100 nM siRNA in cytofectin was added drop wise to the cell culture. Numbers of viable cells were evaluated 48 h after culture, by incubating with Tetra color one (Seikagaku CO., Tokyo, Japan), and numbers obtained were compared with those of controls. Control experiments were performed using Cy3-labeled siRNA (Qiagen) directed against an unrelated mRNA (Luciferase; $siRNA_{LUC}$: Qiagen). Transfection efficiency was confirmed with Cy3-labeled $siRNA_{LUC}$ in each assay. All proliferation experiments were repeated as independent experiments at least twice. Results were reported as means±s.d. of two independent experiments.

Cell invasion of Matrigel

A Transwell containing an 8-μm diameter pore membrane (Becton-Dickinson, Tokyo, Japan) was coated with 500 μl Matrigel (Becton-Dickinson) at 100 μg/ml. Cells were either left untreated, treated with control or DDR1-#1, #2 siRNAs and transfected as described above. After 24-h incubation, cells were detached with cell dissociation solution (Sigma), washed twice with PBS and resuspended in minimum essential medium (MEM) (Nissui Pharmaceutical Inc., Tokyo, Japan) containing 10% fetal bovine serum (FBS) (Gibco, Tokyo, Japan). When siRNAs were used, a second transfection 24 h after the first was performed. In all cases, 2×10^5 cells were seeded into the upper, Matrigel-coated chamber of the Transwell. The lower chamber was filled with MEM supplemented with 10% FBS. After 24-h incubation at 37°C, the non-migrating cells in the upper chamber were gently detached by scraping and adherent cells present on the lower surface of each insert were stained with Giemsa. Ten fields were counted by light microscopy at ×200 magnification. Results were calculated with reference to control values observed after incubation of untreated control, for control and DDR1 siRNA.

Cell lines and culture

All glioma cell lines were cultured in MEM supplemented with 10% FBS. The T98G, GI-1 and U251 cell lines were purchased from Cell Bank, RIKEN BioResource Center (Tsukuba, Japan).

Abbreviations

ALCAM, activated leukocyte cell adhesion molecule; cDNA, complementary DNA; Cy, cyanine; DDR1, discoidin domain receptor family, member 1; DYRK3, dual-specificity tyrosine-(Y)-phosphorylation-regulated kinase 3; FBS, fetal bovine serum; ITGA5, integrin alpha 5; ITGB2, integrin beta 2; KSP37, Ksp37 protein; LDHC, lactate dehydrogenase C; LOC340371, hypothetical protein LOC340371; MEM, minimum essential medium; PBS, phosphate-buffered saline; SLC2A3, solute carrier family 2 member 3; SLN, sarcolipin; s.d., standard deviation; siRNA, short interfering RNA.

Acknowledgements

We are grateful to N Kiyama and F Higuchi for their excellent technical assistance. We thank Dr Rich Simon and Amy Peng for providing the BRB ArrayTools software. The free software was very useful and developed for user-friendly applications. We also thank Tetsutaro Hamano for statistical advices and analysis.

References

Agrawal D, Chen T, Irby R, Quackenbush J, Chambers AF, Szabo M *et al.* (2002). *J Natl Cancer Inst* 94: 513–521.

Freije WA, Castro-Vargas FE, Fang Z, Horvath S, Cloughesy T, Liau LM *et al.* (2004). *Cancer Res* 64: 6503–6510.

Godard S, Getz G, Delorenzi M, Farmer P, Kobayashi H, Desbaillets I *et al.* (2003). *Cancer Res* 63: 6613–6625.

Hoelzinger DB, Mariani L, Weis J, Woyke T, Berens TJ, McDonough WS *et al.* (2005). *Neoplasia* 7: 7–16.

Hunter SB, Brat DJ, Olson JJ, Von Deimling A, Zhou W, Van Meir EG. (2003). *Int J Oncol* 23: 857–869.

Karpeh MS, Kelsen DP, Tepper JE. (2001) In: Devita Jr VT (ed) *Cancer of the Stomach: Cancer, Principles & Practice of Oncology*, 6th edn. Lippincott Williams & Wilkins: Philadelphia, pp 1092–1121.

Khan J, Wei JS, Ringner M, Saal LH, Ladanyi M, Westermann F *et al.* (2001). *Nat Med* 7: 673–679.

Kim S, Dougherty ER, Shmulevich I, Hess KR, Hamilton SR, Trent JM *et al.* (2002). *Mol Cancer Ther* 1: 1229–1236.

Kleihues P, Cavenee WK. (2000). *World Health Organization Classification of Tumours of the Nervous System*. WHO/IARC: Lyon, France.

Li K, Zhao S, Karur V, Wojchowski DM. (2002). *J Biol Chem* 277: 47052–47060.

Liang Y, Diehn M, Watson N, Bollen AW, Aldape KD, Nicholas MK *et al.* (2005). *Proc Natl Acad Sci USA* 102: 5814–5819.

Mischel PS, Cloughesy TF, Nelson SF. (2004). *Nat Rev Neurosci* 5: 782–792.

Mischel PS, Shai R, Shi T, Horvath S, Lu KV, Choe G *et al.* (2003). *Oncogene* 22: 2361–2373.

Nigro JM, Misra A, Zhang L, Smirnov I, Colman H, Griffin C *et al.* (2005). *Cancer Res* 65: 1678–1686.

Nutt CL, Mani DR, Betensky RA, Tamayo P, Cairncross JG, Ladd C *et al.* (2003). *Cancer Res* 63: 1602–1607.

Ogawa K, Tanaka K, Ishii A, Nakamura Y, Kondo S, Sugamura K *et al.* (2001). *J Immunol* 166: 6404–6412.

Ramaswamy S, Tamayo P, Rifkin R, Mukherjee S, Yeang CH, Angelo M *et al.* (2001). *Proc Natl Acad Sci USA* 98: 15149–15154.
Ram R, Lorente G, Nikolich K, Urfer R, Foehr E, Nagavarapu U. (2006). *J Neurooncol* 76: 239–248.
Rickman DS, Bobek MP, Misek DE, Kuick R, Blaivas M, Kurnit DM *et al.* (2001). *Cancer Res* 61: 6885–6891.
Rich JN, Hans C, Jones B, Iversen ES, McLendon RE, Rasheed BK *et al.* (2005). *Cancer Res* 65: 4051–4058.
Sallinen SL, Sallinen PK, Haapasalo HK, Helin HJ, Helen PT, Schraml P *et al.* (2000). *Cancer Res* 60: 6617–6622.
Shai R, Shi T, Kremen TJ, Horvath S, Liau LM, Cloughesy TF *et al.* (2003). *Oncogene* 22: 4918–4923.
Sorlie T, Tibshirani R, Parker J, Hastie T, Marron JS, Nobel A *et al.* (2003). *Proc Natl Acad Sci USA* 100: 8418–8423.
Somasundaram K, Reddy SP, Vinnakota K, Britto R, Subbarayan M, Nambiar S *et al.* (2005). *Oncogene* 24: 7073–7083.
Stewart LA. (2002). *Lancet* 359: 1011–1018.
Stupp R, Mason WP, van den Bent MJ, Weller M, Fisher B, Taphoorn MJ *et al.* (2005). *N Engl J Med* 352: 987–996.
van de Vijver MJ, He YD, van't Veer LJ, Dai H, Hart AA, Voskuil DW *et al.* (2002). *N Engl J Med* 347: 1999–2009.
van't Veer LJ, Dai H, van de Vijver MJ, He YD, Hart AA, Mao M *et al.* (2002). *Nature* 415: 530–536.
van den Boom J, Wolter M, Kuick R, Misek DE, Youkilis AS, Wechsler DS *et al.* (2003). *Am J Pathol* 163: 1033–1043.
Vogel W. (1999). *FASEB J* 13: S77–82.
Vogel W, Brakebusch C, Fassler R, Alves F, Ruggiero F, Pawson T. (2000). *J Biol Chem* 275: 5779–5784.
Weiner HL, Zagzag D. (2000). *Cancer Invest* 18: 544–554.
Wong KK, Chang YM, Tsang YT, Perlaky L, Su J, Adesina A *et al.* (2005). *Cancer Res* 65: 76–84.
Yoshimura T, Matsuyama W, Kamohara H. (2005). *Immunol Res* 31: 219–230.

Cancer Chemother Pharmacol (2005) 56 (Suppl 1): s90–s93
DOI 10.1007/s00280-005-0104-6

Kazuto Nishio · Tokuzo Arao · Tatsu Shimoyama · Yasuhiro Fujiwara · Tomohide Tamura · Nagahiro Saijo

Translational studies for target-based drugs

Published online: 5 November 2005

Abstract The biological background for the clinical and prognostic heterogeneity among tumors within the same histological subgroup is due to individual variations in the biology of tumors. The number of investigations looking at the application of novel technologies within the setting of clinical trials is increasing. The most promising way to improve cancer treatment is to build clinical research strategies on intricate biological evidence. New genomic technologies have been developed over recent years. These techniques are able to analyze thousands of genes and their expression profiles simultaneously. The purpose of this approach is to discover new cancer biomarkers, to improve diagnosis, predict clinical outcomes of disease and response to treatment, and to select new targets for novel agents with innovative mechanisms of action. Gene expression profiles are also used to assist in selecting biomarkers of pharmacodynamic effects of drugs in the clinical setting. Biomarker monitoring in surrogate tissues may allow researchers to assess "proof of principle" of new treatments. Clinical studies of biomarkers monitoring toxicity profiles have also been done. Such pharmacodynamic markers usually respond to treatment earlier than clinical response, and as such may be useful predictors of efficacy. Epidermal growth factor receptor (EGFR) mutation in lung cancer tissues is a strong predictive biomarker for EGFR-targeted protein tyrosine kinase inhibitors. Monitoring of EGFR mutation has been broadly performed in retrospective and prospective clinical studies. However, global standardization for the assay system is essential for such molecular correlative studies. A more sensitive assay for EGFR mutation is now under evaluation for small biopsy samples. Microdissection for tumor samples is also useful for the sensitive detection of EGFR mutation. Novel approaches for the detection of EGFR mutation in other clinical samples such as cytology, pleural effusion and circulating tumor cells are ongoing.

Keywords Biomarker · Proof of principle · Pharmacodynamic marker · EGFR mutation

This work was presented at the 20th Bristol-Myers Squibb Nagoya International Cancer Treatment Symposium, "New Concepts of Treatment Strategies for Hormone-Related Cancer", 11–12 March 2005, Nagoya, Japan.

K. Nishio (✉) · T. Arao · T. Shimoyama
Shien Lab, National Cancer Center Hospital,
Tsukiji 5-1-1, Chuo-ku, 104-0045 Tokyo, Japan
E-mail: knishio@gan2.res.ncc.go.jp
Tel.: +81-3-35422511
Fax: +81-3-35475185

T. Shimoyama · Y. Fujiwara · T. Tamura · N. Saijo
Medical Oncology, National Cancer Center Hospital, Tokyo, Japan

K. Nishio (✉) · T. Arao
Pharmacology Division,
National Cancer Center Research Institute, Tokyo, Japan

Correlative studies at the National Cancer Center Hospital

Molecular correlative studies are essential for the development of anticancer molecular-targeted drugs. One of the major purposes of a correlative study is "proof of principle" (POP). However, clinical POP studies for small molecules are often more difficult to complete than those for antibodies.

Since 2001, the National Cancer Center Hospital (Tokyo, Japan) has been operating as a laboratory for translational studies to develop molecular correlative studies. The laboratory members include medical oncologists, basic researchers, CRC research fellows, invited researchers from abroad, technicians and statisticians. The laboratory is located next to the phase I wards in the hospital, enabling more than ten molecular correlative studies to be simultaneously performed. New clinical samples can be quickly obtained from patients (including outpatients), prepared for storage and stored in the laboratory. The medical doctors

Table 1 Classification of biomarkers and their goals

Biomarker	Goal
Diagnostic markers	
Prognostic markers	
Predictive markers (patient selection)	Selection of patients most likely to benefit from given treatment
Pharmacodynamic markers	Dose finding and schedule
Response and efficacy markers	To measure or infer patient benefit/relate patient benefit to target inhibition
Toxicity prediction markers	

working in the laboratory are often research fellows supported by government grants as these individuals are often interested in this kind of research.

The location of the laboratory also gives frequent opportunities to medical oncologists to communicate with researchers. The significance of study endpoints, study design, technical and statistical information and feasibility are often discussed, especially among young medical oncologists and researchers. As a result, young oncologists and researchers often collaborate in the proposal of new molecular correlative studies.

The major activities of the laboratory are pharmacokinetics and pharmacodynamics studies for early clinical trials (phase I–II) and reverse translational studies. Essentially, "biomarker monitoring" using various biological technologies in these clinical studies are preformed. The selection and validation of biomarkers is a major endpoint for molecular correlative studies. Biomarkers are defined as described in Table 1. Tissue banking and quality control are two of the most important activities. Part of clinical sample testing is performed in collaboration with the Contract Research Organization (CRO) (Fig. 1).

Gene expression profiles

Gene expression array (DNA chips) has been widely used in clinical studies to predict response and in POP studies [3]. Many kinds of DNA chip are now available. Oligonucleotide arrays containing >40,000 genes have recently become popular. These chips can be used differentially depending on the requirements. Before the clinical use, however, an array's quality (linearity and reproducibility) should be determined in preclinical studies. At the National Cancer Center Hospital, the quality of each array is evaluated and expressed as the Pearson's product-moment coefficient of correlation. Based on the validated quality of the cDNA, protocols based on "experienced designs" are then established.

In clinical settings, sample quality and protocol feasibility are often major limitations in the design of new studies. To maintain the quality of clinical samples, a system for sample flow has been established. First, purity of the nucleotides must be carefully examined. Purification methods largely depend on the tumor types. For example, brain tumors contain large amounts of carbohydrate chains, lung cancer samples are sometimes very hard, and breast cancer biopsy samples are lipid rich. These sample characteristics influence the purification quality and efficiency.

After the gene expression profiles have been obtained for each sample, the data are analyzed by standardization, clustering, statistical analysis and validation methods. Statistical and biological validation are essential. Ideally, clinical cross-validation studies should be performed for independent clinical studies. On the other

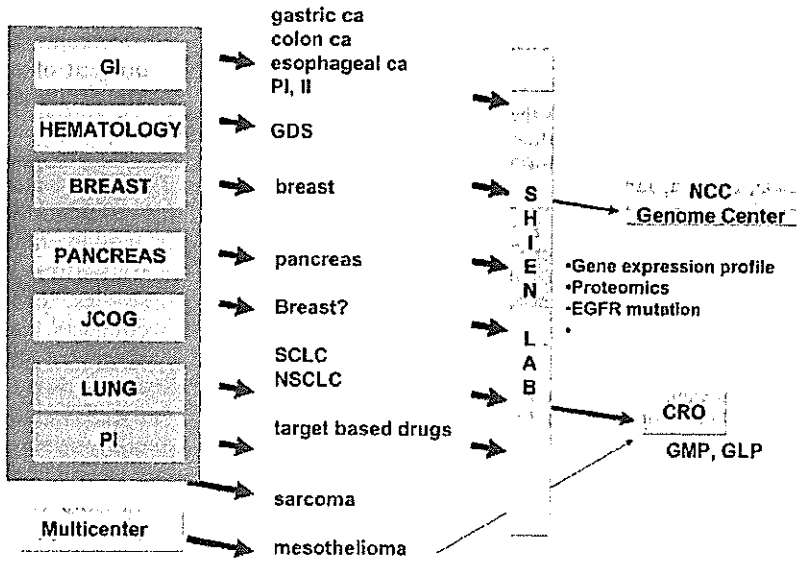

Fig. 1 Flow of clinical samples in molecular correlative studies at the National Cancer Center Hospital. (*GI* gastrointestinal, *JCOG* Japan Clinical Oncology Group, *PI* clinical phase I study, *PII* clinical phase II study, *GDS* gene delivery system, *SCLC* small cell lung cancer, *NSCLC* non-small cell lung cancer, *NCC* National Cancer Center, *CRO* Contact Research Organization, *GMP* Good Manufacturing Practice)

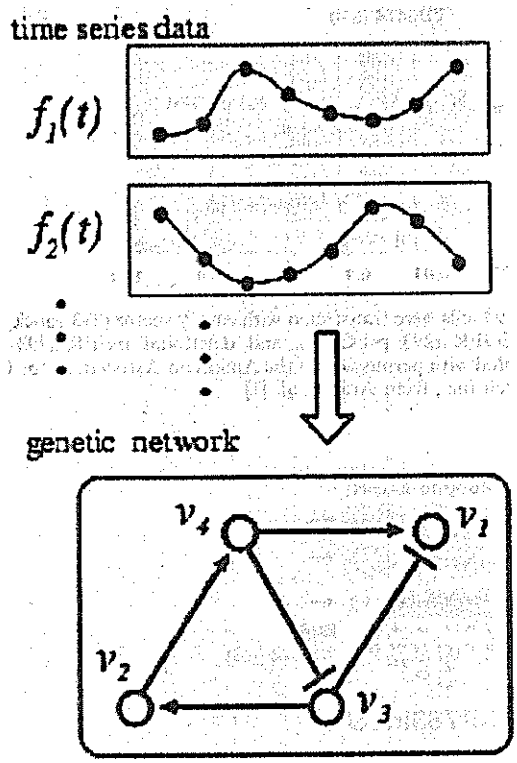

Fig. 2 Network analysis to determine transcriptional pathway and signal transduction pathway modulated by transcriptional regulators and multitarget tyrosine kinase inhibitors using gene expression profiling dataset

hand, biomarkers can be validated in the same clinical study by the "leave-one-out" method. The endpoint of these correlative studies is usually the selection of biomarkers for predicting response or toxicity. For such endpoints, the quality of the clinical study itself is also very important.

We have also used other endpoints in early clinical studies, such as comparing clinical samples obtained before and after the treatment. Analysis of gene alterations after treatment can be utilized to reveal pharmacodynamic effects. We have completed such correlative studies as part of a clinical assessment of multitarget tyrosine kinase inhibitors (TKI), farnesyl transferase inhibitor, and cytotoxic drugs [7].

For biological confirmation, we usually perform real-time RT-PCR and immunostaining. However, we recently discovered that "pathway analysis" is a powerful method for improving our understanding of the alteration of genes related to biological signal transduction pathways. To analyze transcription factors, "network analysis" can be used to identify their signaling pathways (Fig. 2).

Toxicogenomic project for breast cancer

As an approach of gene expression profiling in clinical samples, we monitored gene expression in breast cancer

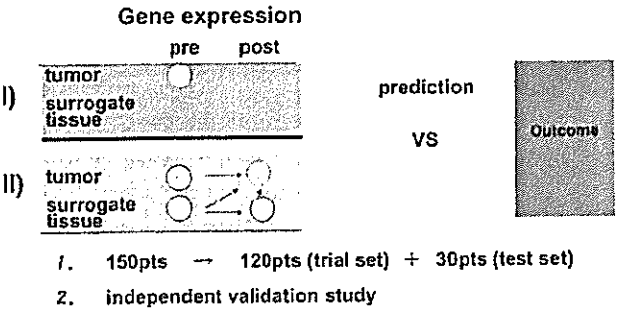

Fig. 3 Gene expression monitoring to distinguish the outcome of treatment for breast cancer patients

patients during treatment with FEC followed by weekly paclitaxel ± trastuzumab in the adjuvant setting. The purpose of this approach was to predict outcomes as well as to study the pharmacodynamic effects of each treatment. Gene expression profiles of peripheral blood mononuclear cells obtained pre- and posttreatment and of tumor biopsy samples obtained pretreatment were determined (Fig. 3). An algorithm to distinguish outcomes using the dataset of these three sampling points was created and expected to be more powerful than conventional outcome assessment techniques.

It seems quite an unusual approach to use normal cells in gene expression profiling in oncology; however, this has proved to be a useful way to monitor drug pharmacodynamic effects and to select biomarkers. Using this approach, we selected biomarkers to capture adverse effects of the treatments. Such "biomarker monitoring" is a rapidly growing field of research.

Biomarker monitoring for tyrosine kinase inhibitors

Recently, EGFR mutation has become an exciting topic in research on TKI [4, 6]. Mutation analysis is now essential for any correlative studies for TKI. Patients with tumors containing the EGFR mutation in different exons are thought to have different responses to TKI. A short, in-frame deletional mutant (E746-A750del) is one of the major mutant forms of EGFR in Japanese populations, and a determinant for EGFR-specific TKI such as gefitinib and ZD6474 (Fig. 4) [1, 8]. We investigated the biological and pharmacological functions of this mutated EGFR to determine whether tumors with deletional-EGFR status are responsive to ligand stimulation, whether mutated EGFR is constitutively active, and whether the downstream intracellular signaling pathway is altered. We concluded that deletional EGFR is constitutively active and that its downstream events are shifted to the AKT pathway (Fig. 5). In addition, a cell-free kinetic assay using mutant EGFR proteins demonstrated differential affinity to TKI among different EGFR mutants. Additional mutations after treatment are also generating interest with regard to their role in acquired resistance to TKI [2]. Thus, the mutation

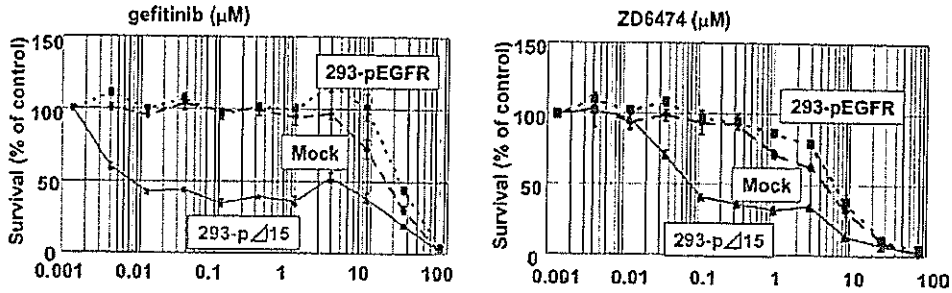

Fig. 4 In vitro sensitivity of 293 cells transfected with a deletional epidermal growth factor receptor (*EGFR*) gene (E746-A750) to tyrosine kinase inhibitors (gefitinib and ZD6474) determined by MTT assay. EGFR mutation (E746-A750 type deletion) increases sensitivity to tyrosine kinase inhibitors (gefitinib and ZD6474). HEK293 cells were transfected with empty vector (293-mock), wild-type EGFR (293 p-EGFR), and deletional EGFR (293-pΔ15). Reprinted with permission of the American Association for Cancer Research Inc., from Arao et al. [1]

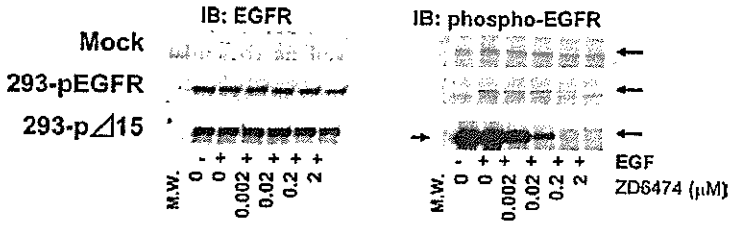

Simple Δ15 *vs* Del L747-P753insS ?

Fig. 5 Constitutive phosphorylation of mutant EGFR. Phosphorylation of EGFR was determined by immunoblotting in 293 cells transfected with Mock, wild-type EGFR, and deletional EGFR cDNA. Increased phosphorylation was observed in the 293-pΔ15 cells under no ligand stimulation. Reprinted with permission of the American Association for Cancer Research Inc., from Arao et al. [1]. (*EGF* epidermal growth factor receptor, *IB* immunoblotting)

status of EGFR is one of the determinants for the prediction of tumor response to EGFR-targeted TKI. On the other hand, the clinical impact of EGFR mutation on survival in patients treated with these TKI remains unclear. Therefore, molecular correlative study including EGFR mutation analysis is quite important for prospective studies. Various technologies for EGFR mutation assay have been developed and some of these assays have been validated in the clinical situation [5]. Gene mutation analysis in prospective studies of TKI using standardized technologies is very important.

Protein arrays

Proteomics technology has been developed and successfully used to identify biomarkers for target-based drugs in a few clinical studies. Additional approaches such as antibody arrays and "PowerBlots®", especially those using phospho-specific antibodies, should enable us to perform "kinome" analyses. Hence, these protein analysis technologies are now powerful tools for research on TKI.

Acknowledgements This work was supported by funds for the Third Term Comprehensive 10-Year Strategy for Cancer Control and a Grant-in-Aid for Scientific Research and for Health and Labour Science Research Grants, Research on Advanced Medical Technology, H14-Toxico-007.

References

1. Arao T, Fukumoto H, Takeda M, Tamura T, Saijo N, Nishio K (2004) Small in-frame deletion in the epidermal growth factor receptor as a target for ZD6474. Cancer Res 64:9101–9104
2. Koizumi F, Shimoyama T, Taguchi F, Saijo N, Nishio K (2005) Establishment of a human non-small cell lung cancer cell line resistant to gefitinib. Int J Cancer 116:36–44
3. Korfee S, Eberhardt W, Fujiwara Y, Nishio K (2005) The role of DNA-microarray in translational cancer research. Curr Pharmacogenomics (in press)
4. Lynch TJ, Bell DW, Sordella R, Gurubhagavatula S, Okimoto RA, Brannigan BW, Harris PL, Haserlat SM, Supko JG, Haluska FG, Louis DN, Christiani DC, Settleman J, Haber DA (2004) Activating mutations in the epidermal growth factor receptor underlying responsiveness of non-small-cell lung cancer to gefitinib. N Engl J Med 350:2129–2139
5. Nishio M, Obyanagi F, Horiike A, Ishikawa Y, Satoh Y, Okumura S, Nakagawa K, Nishio K, Horai T (2005) Gefitinib treatment affects androgen levels in non-small-cell lung cancer patients. Br J Cancer 92:1877–1880
6. Paez JG, Janne PA, Lee JC, Tracy S, Greulich H, Gabriel S, Herman P, Kaye FJ, Lindeman N, Boggon TJ, Naoki K, Sasaki H, Fujii Y, Eck MJ, Sellers WR, Johnson BE, Meyerson M (2004) EGFR mutations in lung cancer: correlation with clinical response to gefitinib therapy. Science 304:1497–1500
7. Shimoyama T, Yamamoto N, Hamano T, Tamura T, Nishio K (2005) Gene expression analysis to identify the pharmacodynamic effects of docetaxel on the Rho signal pathway in human lung cancer patients (abstract 2002). Proc Am Soc Clin Oncol 23:135s
8. Taguchi F, Koh Y, Koizumi F, Tamura T, Saijo N, Nishio K (2004) Anticancer effects of ZD6474, a VEGF receptor tyrosine kinase inhibitor, in gefitinib ("Iressa")-sensitive and resistant xenograft models. Cancer Sci 95:984–989

Enhancement of Sensitivity to Tumor Necrosis Factor α in Non–Small Cell Lung Cancer Cells with Acquired Resistance to Gefitinib

Koichi Ando,[1] Tohru Ohmori,[1,2] Fumiko Inoue,[2] Tsuyoki Kadofuku,[2] Takamichi Hosaka,[1] Hiroo Ishida,[1] Takao Shirai,[1] Kentaro Okuda,[1] Takashi Hirose,[1] Naoya Horichi,[1] Kazuto Nishio,[3] Nagahiro Saijo,[3] Mitsuru Adachi,[3] and Toshio Kuroki[4]

Abstract Tumor cells that have acquired resistance to gefitinib through continuous drug administration may complicate future treatment. To investigate the mechanisms of acquired resistance, we established PC-9/ZD2001, a non-small-cell lung cancer cell line resistant to gefitinib, by continuous exposure of the parental cell line PC-9 to gefitinib. After 6 months of culture in gefitinib-free conditions, PC-9/ZD2001 cells reacquired sensitivity to gefitinib and were established as a revertant cell line, PC-9/ZD2001R. PC-9/ZD2001 cells showed collateral sensitivity to several anticancer drugs (vinorelbine, paclitaxel, camptothecin, and 5-fluorouracil) and to tumor necrosis factor α (TNF-α). Compared with PC-9 cells, PC-9/ZD2001 cells were 67-fold more sensitive to TNF-α and PC-9/ZD2001R cells were 1.3-fold more sensitive. Therefore, collateral sensitivity to TNF-α was correlated with gefitinib resistance. PC-9/ZD2001 cells expressed a lower level of epidermal growth factor receptor (EGFR) than did PC-9 cells; this down-regulation was partially reversed in PC-9/ZD2001R cells. TNF-α-induced autophosphorylation of EGFR (cross-talk signaling) was detected in all three cell lines. However, TNF-α-induced Akt phosphorylation and IκB degradation were observed much less often in PC-9/ZD2001 cells than in PC-9 cells or PC-9/ZD2001R cells. Expression of the inhibitor of apoptosis proteins c-IAP1 and c-IAP2 was induced by TNF-α in PC-9 and PC-9/ZD2001R cells but not in PC-9/ZD2001 cells. This weak effect of EGFR on Akt pathway might contribute to the TNF-α sensitivity of PC-9/ZD2001 cells. These results suggest that therapy with TNF-α would be effective in some cases of non-small-cell lung cancer that have acquired resistance to gefitinib.

Gefitinib (Iressa, ZD1839), a small-molecule epidermal growth factor receptor (EGFR) tyrosine kinase inhibitor, has been approved for the treatment of refractory and relapsed non-small-cell lung cancer (NSCLC) patients in a number of countries around the world. This drug, which is given continuously as a once-daily oral dose, showed antitumor activity in patients with relapsed or recurrent NSCLC; however, tumor responses were observed in 12% to 18% of patients with chemotherapy-refractory advanced NSCLC (1, 2). Even in cases sensitive to gefitinib, resistance might be acquired through continuous drug administration. Additional treatments for cases of NSCLC relapsing during treatment with gefitinib are urgently needed.

To investigate the mechanism of acquired resistance to gefitinib, we previously established gefitinib-acquired resistant cells, PC-9/ZD2001, from a NSCLC, PC-9, which is hypersensitive to gefitinib and has a 15-del mutation in exon 19 of EGFR (data not shown). After >6 months of culture in gefitinib-free conditions, the sensitivity of PC-9/ZD2001 cells to gefitinib was restored, and the cells were subsequently established as a revertant cell line, PC-9/ZD2001R. The active mutation of EGFR was sustained in both the resistant and the revertant cell lines and the existence of revertant cell line suggests the additional mutation of EGFR, such as a secondary mutation of T790M in EGFR that causes resistance to gefitinib (3, 4), is unlikely to be contribute to this gefitinib resistance. In the gefitinib-resistant cells, the expression levels of EGFR and mRNA decreased to 30% to 50% of those in parental cells. A ligand-induced EGFR activation minimally activated mitogen-activated protein kinase signaling pathways and the inhibitory effect of gefitinib on this

Authors' Affiliations: [1]First Department of Internal Medicine and [2]Institute of Molecular Oncology, Showa University, Tokyo, Japan; [3]Internal Medicine, Pharmacology Division, National Cancer Center Hospital, National Cancer Center Research Institute, Tokyo, Japan; and [4]Gifu University, Gifu, Japan
Received 4/12/05; revised 8/10/05; accepted 8/26/05.
Grant support: Grant-in-Aid for a High-Technology Research Center Project from the Ministry of Education, Science, Sports, and Culture of Japan; Showa University Grant-in-Aid for Innovative Collaborative Research Projects; and Special Research Grant-in-Aid for Development of Characteristic Education from the Ministry of Education, Culture, Sports, Science, and Technology of Japan.
The costs of publication of this article were defrayed in part by the payment of page charges. This article must therefore be hereby marked *advertisement* in accordance with 18 U.S.C. Section 1734 solely to indicate this fact.
Requests for reprints: Tohru Ohmori, Institute of Molecular Oncology, Showa University, Hatanodai, 1-5-8, Shinagawa-ku, Tokyo 142-8555, Japan. Fax: 81-3-3784-2299; E-mail: ohmorit@med.showa-u.ac.jp.

doi:10.1158/1078-0432.CCR-05-0811

pathway was significantly decreased in the resistant cells.[5] To elucidate the cross-resistance to other anticancer agents, we examined the sensitivity to the conventional anticancer agents and tumor necrosis factor α (TNF-α). PC-9/ZD2001 showed cross-resistance to another EGFR inhibitor, AG1478. Interestingly, gefitinib-resistant cells were ~3-fold more sensitive than PC-9 cells to the cytotoxic effects of vinorelbine, paclitaxel, camptothecin, 5-fluorouracil, and a cytokine, TNF-α.[5] The same tendency was confirmed in the other gefitinib-resistant clones established along with PC-9/ZD2001. The restoration of these collateral sensitivities (except 5-fluorouracil) in revertant PC-9/ZD2001R cells suggests that such sensitivities are correlated with the mechanism of gefitinib resistance.

TNF-α is the prototype of ~20 related cytokines that act through specific members of the TNF receptor (TNFR) super family (5–7). Several cancer therapies exploiting the cytotoxic effect of TNF-α on solid tumors and soft-tissue sarcomas have recently been examined in clinical trials (8, 9). The TNF-α stimulates inflammation by turning on gene transcription through signaling cascades such as the Akt/nuclear factor κB (NF-κB) pathway. This signaling subsequently serves as the primary mechanism to protect cells against apoptotic stimuli through several transcriptional genes, such as inhibitor of apoptosis proteins (IAP), the specific inhibitor of caspases (10, 11). In contrast, TNF-α-mediated signaling also triggers apoptosis through the activation of caspase-8 and the downstream caspase-3 or caspase-7 in a wide variety of cells (12). From these observations, it is possible to say that TNF-α has two different signaling pathways that contradict each other. The cytotoxic effect of TNF-α might be determined by ratios between the apoptosis-inducing and the apoptosis-inhibiting effects.

Akt/NF-κB signaling also occurs downstream of EGFR and this signaling mediates cell proliferation and antiapoptotic signaling through this pathway (13). In the case of the antiapoptotic signaling of TNF-α, TNFR is known to activate Akt/NF-κB in three ways: directly through phosphatidylinositol 3-kinase activation, or indirectly through cross-talk signaling to EGFR, or both together (5–7, 12, 14, 15). Moreover, several recent articles report that the TNFR-mediated cross-talk signaling to EGFR occurs in a ligand-dependent and -independent manner (16–21). Therefore, to investigate the mechanisms of the collateral sensitivity to TNF-α in gefitinib-acquired resistant cells, we focused on TNF-α-induced cross-talk signaling to EGFR and analyzed the Akt/NF-κB signaling pathway in response to TNF-α.

In this article, we show that a weakness of Akt/NF-κB signaling from TNF-α-mediated cross-talk signaling via EGFR causes the collateral sensitivity to TNF-α in the gefitinib-acquired resistant cell line. Moreover, this cross-talk signaling is thought to be a dominant pathway of TNF-α-mediated Akt activation.

Materials and Methods

Chemicals and antibodies. Gefitinib was donated by AstraZeneca Pharmaceuticals (Wilmington, DE). An anti-phospho-EGFR antibody (Tyr1068) was purchased from Cell Signaling Technology (Beverly, MA). Other antibodies and chemicals were purchased from Santa Cruz Biotechnology, Inc. (Santa Cruz, CA) and Sigma-Aldrich Co. (St. Louis, MO), respectively, unless otherwise specified.

Cell lines and cultures. The PC-9 human NSCLC cell line, established from a previously untreated patient, was kindly donated by Prof. K. Hayata (Tokyo Medical College, Tokyo, Japan.). The PC-9 cells were cultured with RPMI 1640 supplemented with 10% FCS and maintained in a 5% CO_2 incubator at 37°C under humidified conditions.

Establishment of gefitinib-resistant cell lines. To establish gefitinib-resistant cell lines, PC-9 cells were continuously exposed to increasing dosages of gefitinib for >1 year. The surviving cells were cloned and three gefitinib-resistant cell lines, designated as PC-9/ZD2001, PC-9/ZD2002, and PC-9/ZD2003, were established. These cell lines can survive exposure to 200 nmol/L gefitinib. Sensitivity to gefitinib was restored by culture of PC-9/ZD2001 in gefitinib-free conditions for >6 months. The restored cells were cloned and subsequently established as a revertant cell line, PC-9/ZD2001R.

Established resistant cell lines were maintained by culture in a medium containing 200 nmol/L gefitinib. To eliminate the effects of gefitinib, the resistant cells were cultured in a drug-free medium for at least 2 weeks before all experiments. As the relative resistance values of these cell lines were stable for at least 3 months after culture under drug-free conditions (data not shown), we used the cells for experiments during this period.

Growth inhibition assay. To measure sensitivity to gefitinib, a 3-(4,5-dimethylthiazol-2-yl)-2,5-diphenyltetrazolium bromide assay was done (Cell Titer 96 assay kit, Promega Corp., Madison, WI). In brief, PC-9, PC-9/ZD2001, and PC-9/ZD2001R cells were seeded onto 96-well plates and preincubated overnight. The cells were continuously exposed to the indicated concentrations of gefitinib for 4 or 5 days. Absorbance was measured at 570 nm with a microplate reader (Model 550, Bio-Rad Laboratories, Hercules, CA).

Analysis of tumor necrosis factor α–induced apoptotic cell death. The PC-9, PC-9/ZD2001, and PC-9/ZD2001R cells were treated with 100 ng/mL TNF-α for the indicated time periods. They were then fixed with 4% paraformaldehyde at 4°C for 30 minutes. After 100 μL of 70% ethanol were added, the cells were permeabilized by incubation overnight at −20°C. Apoptotic DNA fragments were probed with the terminal deoxyribonucleotidyl transferase-mediated dUTP nick end labeling method (MEBSTAIN Apoptosis TUNEL Kit Direct, Medical & Biological Laboratories, Nagoya, Japan) and subpopulations of apoptotic cells were measured with a flow cytometer (FACSCalibur, BD Biosciences Immunocytometry Systems, San Jose, CA).

Activity assays for CPP32/caspase-3 and FLICE/caspase-8. Activities of CPP32/caspase-3 and FLICE/caspase-8 were measured with caspase-3 and caspase-8 colorimetric assay kits (MRL Diagnostics, Cypress, CA) according to the instructions of the manufacturer. The PC-9, PC-9/ZD2001, and PC-9/ZD2001R cells were incubated for 12 hours with 10 ng/mL TNF-α and then resuspended in 50 μL of chilled cell lyses buffer. The cells were incubated on ice for 10 minutes and the protein concentration of the supernatant was assayed with a bicinchoninic acid protein assay kit (Sigma-Aldrich). A certain amount of each sample was added to 50 μL of 2× reaction buffer containing the respective substrates DEVD-pNA and IETD-pNA, then incubated at 37°C for 1 hour. After incubation, absorbance was measured at 400 and 405 nm with a microtiter plate reader (Model 550, Bio-Rad Laboratories).

Immunoblot analysis. Cells were treated with 10 ng/mL of TNF-α for 30 minutes, then washed twice with ice-cold PBS and lysed in EBC buffer [50 mmol/L Tris-HCl (pH 8.0), 120 mmol/L NaCl, 0.5% NP40, 100 μmol/L NaF, 200 μmol/L Na orthovanadate, and 10 μg/mL of leupeptin, aprotinin, and phenylmethylsulfonyl fluoride] with an ultrasonic disrupter (Tomy Digital Biology Co., Ltd., Tokyo, Japan). The cell lysate was precleared by centrifugation, resolved by 10% SDS-PAGE, transferred to nitrocellulose membrane, and probed with antibodies against EGFR, phospho-EGFR (Tyr1045), phosphatase and tensin homologue, Akt, phospho-Akt, IκB, c-IAP1, and c-IAP2. Bound antibodies were detected with horseradish peroxidase-linked immunoglobulin (Amersham Biosciences, Buckinghamshire, United Kingdom)

[5] T. Yamaoka, T. Ohmori, F. Inoue, et al. Characteristics of gefitinib-acquired resistance in non–small cell lung cancer cell lines, submitted for publication.

and enhanced chemiluminescence reagents (Perkin-Elmer Life and Analytical Sciences, Boston, MA).

Real-time reverse transcription-PCR method. Total RNA was isolated with the guanidium isothiocyanate method using an RNA purification kit (RNeasy Mini Kit, Qiagen, Venlo, the Netherlands) according to the instructions of the manufacturer. After RNA isolation, cDNA was prepared in the presence of random 9-mers with a reverse transcription-PCR (RT-PCR) kit (Takara Shuzo Co., Ltd., Kyoto, Japan). Expression levels of EGFR, c-IAP1, and c-IAP2 mRNA were quantified with a fluorescence-based real-time detection method (GeneAmp 5700 Sequence Detection System, Applied Biosystems, Foster City, CA). Cycling conditions were 40 cycles at 94°C for 20 seconds, 55°C (EGFR) and 64°C (c-IAPs) for 20 seconds, and 72°C for 30 seconds. Expression of the mRNA was measured with the following primer sets: EGFR, 5′-ACGAATGGGCCTAAGATC-3′ and 5′-TGCTTACCCGGATTCTAGG-3′; c-IAP1, 5′-ATGTGGGTAACAGTGATGATGTCA-3′ and 5-AAACCAC-TTGGCATGTTGAAC-3′; and c-IAP2, 5′-CTAGTGTTCATGTTGAAC-3′ and 5′-CCTCAAGCCACCATCACAAC-3′. The expression of β-actin mRNA was used as an internal control.

Statistical analysis. Statistical analysis was done with the StatView II software program (Abacus Concepts, Berkeley, CA). Activities of CPP32/caspase-3 and FLICE/caspase-8 were analyzed with paired Student's t test. $P < 0.05$ was considered significant.

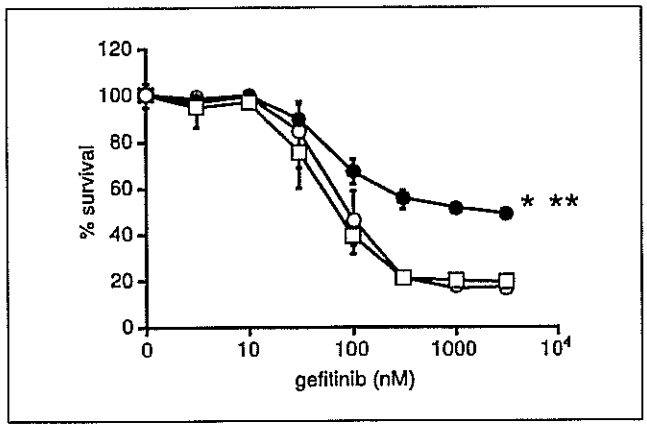

Fig. 1. Cytotoxic effects of gefitinib in a gefitinib-resistant NSCLC cell line. The cells (2×10^3 per well) were seeded onto a 96-well plate and preincubated overnight, then continuously exposed to the indicated concentrations of gefitinib for 4 or 5 days. The growth inhibition rate was analyzed with 3-(4,5-dimethylthiazol-2-yl)-2,5-diphenyltetrazolium bromide assay as described in Materials and Methods. ○, PC-9; ●, PC-9/ZD2001; □, PC-9/ZD2001R. Points, mean of three different experiments; bars, SD. *, $P < 0.001$, PC-9 versus PC-9/ZD2001; **, $P < 0.001$, PC-9/ZD2001R versus PC-9/ZD2001.

Results

Establishment of acquired gefitinib-resistant cell lines. To elucidate the mechanism of acquired resistance against gefitinib, we established gefitinib-resistant NSCLC cell lines through continuous exposure of this drug. Resistance against gefitinib developed quite slowly; the relative resistant values of 3- to 4-fold were reached after >1-year exposure to gefitinib. We picked the clones of gefitinib-resistant cell lines named PC-9/ZD2001, PC-9/ZD2002, and PC-9/ZD2003. These cell lines can survive in 200 nmol/L gefitinib-contained medium. Sensitivities to gefitinib were measured by 3-(4,5-dimethylthiazol-2-yl)-2,5-diphenyltetrazolium bromide assay. In the case of PC-9/ZD2001 cells, the cell line was able to survive by >50% at the concentration of >500 nmol/L gefitinib. This concentration caused maximum inhibition in PC-9. The IC_{40} value of gefitinib in PC-9 cells was 53.0 ± 8.1 nmol/L. The gefitinib-resistant cell line PC-9/ZD2001 showed a 4-fold higher resistance to gefitinib than PC-9 cells (IC_{40} = 211.1 ± 32.4 nmol/L; Fig. 1). Culture of the cells in gefitinib-free conditions for 6 months restored sensitivity to gefitinib in PC-9/ZD2001 and subsequently established a revertant cell line, PC-9/ZD2001R, in which sensitivity to gefitinib was completely restored (IC_{40} = 46.3 ± 10.2 nmol/L).

Analysis for tumor necrosis factor α–induced apoptotic cell death. TNF-α-induced cytotoxic effect was measured by 3-(4,5-dimethylthiazol-2-yl)-2,5-diphenyltetrazolium bromide assay. The IC_{40} values of TNF-α in PC-9, PC-9/ZD2001, and PC-9/ZD2001R cell lines were 815.0 ± 44.8, 12.2 ± 1.4, and 626.2 ± 18.5 ng/mL, respectively. PC-9/ZD2001 cells acquired new sensitivity to TNF-α. PC-9/ZD2001 was ~67-fold more sensitive to TNF-α as compared with PC-9, but this sensitization was restored to 1.3-fold in PC-9/ZD2001R (Fig. 2A). This collateral sensitivity to TNF-α was confirmed in the other gefitinib-resistant cell lines, PC-9/ZD2002 and PC-9/ZD2003 (data not shown).

Additionally, we measured TNF-α-induced apoptotic cell death by flow cytometry. The apoptotic cells were stained by the terminal deoxyribonucleotidyl transferase-mediated dUTP nick end labeling method. No significant apoptosis was observed in these three cell lines until 24 hours of exposure to TNF-α (10 ng/mL). Forty-eight hours of TNF-α exposure induced a 6-fold higher apoptotic cell death in PC-9/ZD2001 cells (70.3%) as compared with the parental PC-9 cells (11.8%). This enhancement was completely recovered in PC-9/ZD2001R cells (16.6%; Fig. 2B; Table 1). These results suggest that the collateral sensitivity to TNF-α might be correlated with the resistance to gefitinib in these cell lines.

Analysis of tumor necrosis factor α–mediated activations of CPP/caspase-3 and FLICE/caspase-8. To clarify the difference of TNF-α-induced apoptotic cell death in these cell lines, we analyzed TNF-α-mediated CPP32/caspase-3 and its upstream FLICE/caspase-8 activations by caspase-8 and caspase-3 colorimetric protease assay kits (Medical and Biological Laboratories), respectively. PC-9, PC-9/ZD2001, and its revertant PC-9/ZD2001R cells were incubated with the indicated concentrations of TNF-α for 12 hours. In the case of caspase-3, TNF-α did not cause any increases in the activity in PC-9 and PC-9/ZD2001R cells even at the highest concentration of 100 ng/mL. In contrast, TNF-α significantly enhanced caspase-3 activity in PC-9/ZD2001 cells even at the concentration of 1 ng/mL within this time course (Fig. 3A). In the case of caspase-8, TNF-α enhanced the activities in all three cell lines from 10 ng/mL (Fig. 3B). TNF-α at 100 ng/mL activated caspase-8 ~1.6-, 2.9-, and 1.9-fold higher in PC-9, PC-9/ZD2001, and PC-9/ZD2001R, as compared with the respective untreated cells. In PC-9/ZD2001 cells, TNF-α caused the highest relative induction of caspase-8 (Fig. 3B).

Immunoblot analysis for the tumor necrosis factor α–induced cross-talk signaling to epidermal growth factor receptor and Akt/nuclear factor κB pathway activation. EGFR expression was significantly lower in PC-9/ZD2001 than in PC-9 cells (Fig. 4A). When measuring the expression of EGFR protein by a densitometer (calculated by the NIH image software), the expression was decreased to 52.4 ± 2.6% of that in parental cell line. Moreover, we measured the expression levels of EGFR mRNA by a real-time RT-PCR method. The expression level in PC-9/ZD2001 was decreased to 37.0 ± 3.2% of that in parental

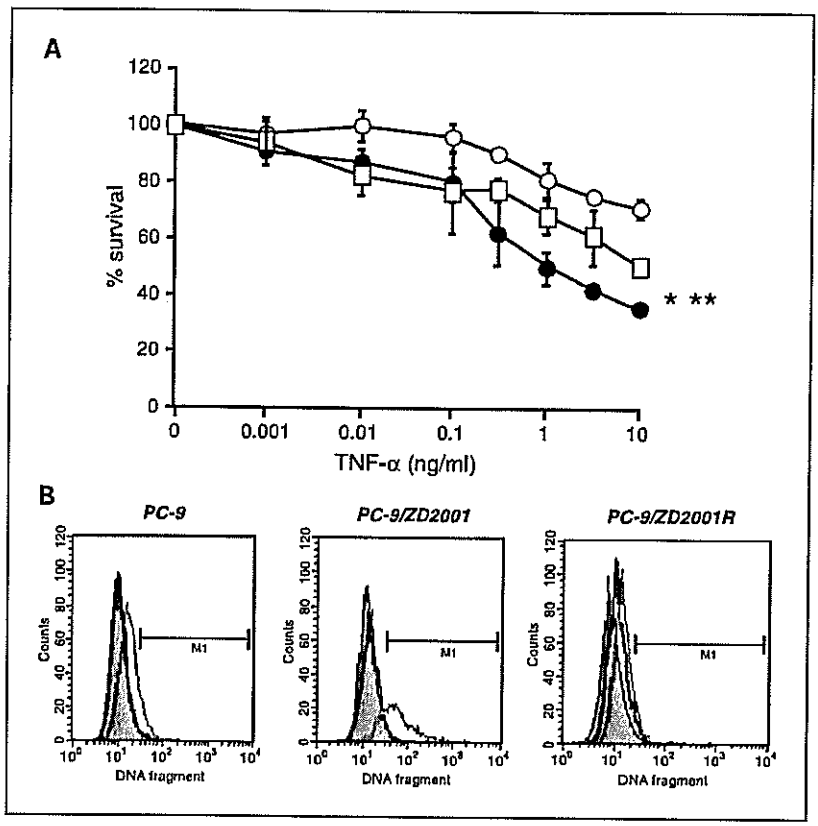

Fig. 2. Gefitinib-resistant cells acquired sensitivity toTNF-α. *A*, the cells were continuously treated with the indicated concentrations of TNF-α for 4 or 5 days. The growth inhibition rate was analyzed with 3-(4,5-dimethylthiazol-2-yl) -2,5-diphenyltetrazolium bromide assay as described in Materials and Methods. ○, PC-9; ●, PC-9/ZD2001; □, PC-9/ZD2001R. PC-9/ZD2001 cells were ~67-fold more sensitive toTNF-α than were PC-9 cells but the sensitivity of revertant PC-9/ZD2001R cells decreased to 1.3-fold that in PC-9 cells. Points, mean of three different experiments; bars, SD. *, $P < 0.001$, PC-9 versus PC-9/ZD2001, **, $P < 0.001$, PC-9/ZD2001R versus PC-9/ZD2001. *B*, the cells were treated with 10 ng/mL TNF-α for the indicated time periods. After treatment, the cells were fixed with 4% paraformaldehyde at 4°C and permeabilized with 70% ethanol. Fragments of apoptotic DNA were stained with the terminal deoxyribonucleotidyl transferase-mediated dUTP nick end labeling method and measured with flow cytometry as described in Materials and Methods.

cells. The same down-regulation of EGFR was seen in the other resistant cell lines (data not shown). In the case of PC-9/ZD2001R, expression levels of EGFR protein and mRNA were also decreased to 69.3 ± 1.1% and 56.8 ± 2.2%, respectively, as compared with PC-9. The expression of EGFR was restored, but not completely, in the revertant cell line.

In PC-9 cells, cross-talk signaling from TNFR to EGFR was observed and treatment with 10 ng/mL TNF-α for 30 minutes induced significant autophosphorylation of EGFR (Fig. 4A). According to the autophosphorylation of EGFR, definite phosphorylation of Akt and a decrease in IκB content were observed. The activation of Akt and down-regulation of IκB were inhibited by gefitinib at concentrations <10 nmol/L. Because gefitinib (100 nmol/L) mostly inhibited this signaling, we concluded that the cross-talk signaling from TNFR to EGFR might be the dominant pathway of TNF-α-mediated Akt/NF-κB activation in this cell line rather than the direct signaling from TNFR to Akt. In contrast, although EGFR autophosphorylation was observed, only partial phosphorylation of Akt and down-regulation of IκB, compared with those in PC-9, were observed after TNF-α exposure in PC-9/ZD2001 cells (Fig. 4A and B). Treatment with gefitinib inhibited this cross-talk signaling to EGFR but had no effect on downstream Akt phosphorylation.

These observations suggest that TNF-α-mediated EGFR signaling has less effect on the Akt/NF-κB pathway in the gefitinib-resistant PC-9/ZD2001 cell line. Other stimuli might activate Akt in an EGFR-independent manner. In the revertant PC-9/ZD2001R cell line, this weak effect of EGFR was largely reversed and TNF-α exposure induced autophosphorylation of EGFR and subsequent activation of the Akt/NF-κB pathway. The expression levels of phosphatase and tensin homologue, a suppressor of Akt signaling, did not differ significantly among PC-9, PC-9/ZD2001, and PC-9/ZD2001R cells. This decreased effect of EGFR might be partially caused by the down-regulation of EGFR expression in PC-9/ZD2001. However, although the EGFR-mediated signaling and the resistance to gefitinib were mostly restored, EGFR expression remained only partially restored in PC-9/ZD2001R. For this reason, we speculated that the down-regulation of EGFR expression might not fully explain the weak EGFR signaling to Akt pathway in PC-9/ZD2001 cells.

To clarify the decreased EGFR signaling in PC-9/ZD2001, we examined the inhibitory effect of a phosphatidylinositol 3-kinase inhibitor, wortmannin, on the TNF-α-induced activation of this pathway (Fig. 4B). Interestingly, wortmannin inhibited the TNF-α-mediated phosphorylation of Akt in PC-9/ZD2001 cells at the same level as it did in PC-9 and PC-9/ZD2001R cells.

Expresstion of c-IAP1 and c-IAP2 on treatment with tumor necrosis factor α. After treatment with TNF-α (10 ng/mL) for 30 minutes, expression of c-IAP1 and c-IAP2 proteins was

Table 1. Percentage of apoptotic subpopulations

%Apoptosis	PC-9	PC-9/2001	PC-9/2001R
Control	1.1	1.2	1.1
24 h	1.4	2.3	3.2
48 h	11.8	70.3	6.6

NOTE: After 72 hours of exposure to TNF-α, significant apoptotic cell death was observed in PC-9/ZD2001 cells but not in PC-9 or PC-9/ZD2001R cells.

significantly increased in PC-9 and PC-9/ZD2001R cells but not in PC-9/ZD2001 cells (Fig. 4A and B). According to the results of Akt phosphorylation, induction was inhibited by gefitinib in PC-9 and PC-9/ZD2001R cells but not in PC-9/ZD2001 cells. Wortmannin could inhibit induction in all three cell lines. Consistent with the results of protein expression, treatment with TNF-α increased the expression level of c-IAP1 and c-IAP2 mRNA in PC-9 and PC-9/ZD2001R cells in a dose-dependent manner (Fig. 5A and B). After treatment with 100 ng/mL TNF-α for 12 hours, the expression levels of both c-IAP1 and c-IAP2 mRNA were significantly increased in PC-9 cells (c-IAP1, 7.05 ± 0.62; c-IAP2, 18.22 ± 0.25) and PC-9/ZD2001R cells (c-IAP1, 7.02 ± 0.54; c-IAP2, 11.56 ± 0.75) but not in PC-9/ZD2001 cells (c-IAP1, 2.60 ± 0.58; c-IAP2, 2.83 ± 0.66). These observations suggest that TNF-α-induced apoptotic signaling is not inhibited by its own antiapoptotic effects, such as IAPs induction, owing to the weak effect of TNF-α-mediated signaling and the Akt/NF-κB pathway via EGFR in this gefitinib-resistant cell line.

Discussion

We have shown that the gefitinib-acquired resistant NSCLC cell line PC-9/ZD2001 acquired collateral sensitivity to the apoptotic effect of TNF-α. Because this collateral sensitivity was significantly diminished in the revertant PC-9/ZD2001R, it might be correlated with gefitinib resistance. As described before, PC-9/ZD2001 also acquired collateral sensitivities to some anticancer drugs, such as vinorelbine, paclitaxel, camptothecin, and 5-fluorouracil. However, this cell line did not show the collateral sensitivities to cisplatin, etoposide, mitomycin C, and cyclophosphamide.[5] Moreover, there was no difference of susceptibility to serum-starved condition between PC-9 and PC-9/ZD2001 (data not shown). From these observations, it can be concluded that the collateral sensitivities of the gefitinib-resistant cells are specific to some cell stresses and are not caused by the fragility of the cells. Because the same tendency of sensitivity was seen in the other resistant clones, PC-9/ZD2002 and PC-9/ZD2003, the acquired sensitivity to the anticancer drugs and TNF-α could be a general phenomenon even in the clinical gefitinib-resistant cells.

TNF-α activates not only apoptotic signaling but also antiapoptotic signaling via the Akt/NF-κB activation (22, 23). Activation of the downstream transcription factor NF-κB inhibits various types of apoptotic cell death by inducing apoptotic inhibitory proteins (22, 23), such as bcl-2 (24), bcl-xl (25), forkhead (26), and IAPs (10, 11, 27, 28). As described before, it is thought that the cytotoxic effect of TNF-α is determined by ratios between the apoptosis-inducing and the apoptosis-inhibiting effects (5–7, 12, 14, 15).

In parental PC-9 cells, TNF-α induced EGFR autophosphorylation and subsequent Akt/NF-κB pathway activation (Fig. 4A and B). This autophosphorylation was completely inhibited by a low concentration of gefitinib (10 nmol/L). From these observations, we think that TNF-α-induced Akt/NF-κB pathway activation occurs mainly through cross-talk from TNFR to EGFR in this cell line. Because the expression level of EGFR was significantly decreased in PC-9/ZD2001 as compared with the parental PC-9, the decline of the cross-talk signaling might partially diminish the TNF-α-induced activation of the Akt/NF-κB pathway. Our results are supported by those of an earlier study showing that resistance to the cytotoxic effect of TNF-α is associated with high expression of Her family receptors, such as EGFR (Her1), erbB2/Her2/neu, or Her3, in a panel of human tumor cell lines (29). However, the decreased EGFR signaling from the Akt/NF-κB pathway could not be fully explained by the lower EGFR expression in PC-9/ZD2001 because EGFR expression remained only partially restored in the revertant PC-9/ZD2001R cell line. In light of these observations, to clarify the mechanisms of collateral sensitivity to TNF-α in the gefitinib-resistant cells, we focused on the cross-talk signaling from TNFR to EGFR in PC-9, PC-9/ZD2001, and PC-9/ZD2001R cells.

Several recent articles have reported that TNFR mediates cross-talk signaling to EGFR through a ligand-dependent and -independent manner (16–19, 21, 23). Chan et al. (17) have reported that exposure of human mammary epithelial cells to TNF-α results in transactivation of EGFR through metalloprotease-dependent shedding of EGFR ligand(s). Hirota et al. (18) reported that EGFR transactivation by TNF-α is

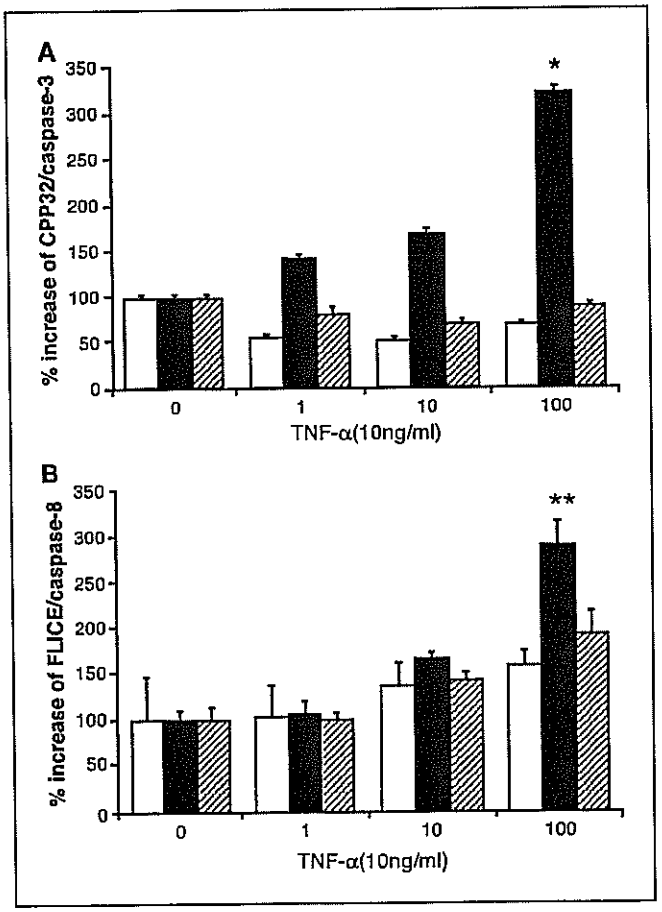

Fig. 3. TNF-α-mediated activation of CPP32/caspase-3 and FLICE/caspase-8 in PC-9, PC-9/ZD2001, and PC-9/ZD2001R cells. Activation of CPP32/caspase-3 and FLICE/caspase-8 was measured as described in Materials and Methods. The cells were exposed to the indicated concentrations of TNF-α for 12 hours; after which equivalent amounts of samples were reacted with the substrates DEVD-pNA and IETD-pNA. Absorbance was measured at 400 and 405 nm with a microtiter plate reader. *A*, CPP32/caspase-3. *B*, FLICE/caspase-8. TNF-α activated FLICE/caspase-8 in all three cell lines but activated CPP32/caspase-3 only in PC-9/ZD2001 cells. Data calculated as the percentage increase compared with respective untreated controls. Points, mean of three different experiments each done in triplicate; bars, SD. Open columns, PC-9; closed columns, PC-9/ZD2001; hatched columns, PC-9/ZD2001R. *, $P < 0.001$, PC-9 versus PC-9/ZD2001. **, $P = 0.02$, PC-9 versus PC-9/ZD2001.

regulated by means of redox-dependent mechanisms. The transactivation of EGFR was observed to occur quickly, after <30 minutes of exposure to TNF-α in PC-9 cells (Fig. 4A and B). No additional induction of ligands, EGF and transforming growth factor-α, were detected by ELISA in the culturing medium of the cells even after 6 hours of 100 ng/mL TNF-α exposure (data not shown). From these observations, we think that this activation could occur independently of ligands but not through TNF-α-mediated ligands synthesis or proteolytic releasing of preexisting ligands from the disrupted cells. Although TNF-α induced the same levels of EGFR autophosphorylation in all three cell lines, this EGFR activation is minimally transmitted to the downstream Akt/NF-κB pathway in the resistant PC-9/ZD2001 cells (Fig. 4A). Moreover, an inhibitory effect of gefitinib on TNF-α-induced Akt/NF-κB activation was not observed although wortmannin, a phosphatidylinositol 3-kinase inhibitor, completely inhibited this signaling in PC-9/ZD2001 cells (Fig. 4B). These results suggest that the weak effect of EGFR on Akt/NF-κB signaling could occur between EGFR and phosphatidylinositol 3-kinase in PC-9/ZD2001 cells.

Several articles reported that the sensitivity to gefitinib is regulated by active mutant EGFR (30, 31), by the expression level of phosphatase and tensin homologue/MMAC/TEP (32), and by levels of Akt phosphorylation (13, 33, 34). Because the gefitinib-hypersensitive PC-9 cells originally had 15-bp deletion mutation in exon 19 of EGFR, they were thought to have a gefitinib-sensitive active mutant EGFR (35); however, because we found no alteration of the EGFR mRNA sequence in PC-9/ZD2001 cells (data not shown), we conclude that this gefitinib-resistant cell line was a good model for acquired gefitinib resistance. In our previous study, EGFR signaling mediated by transforming growth factor-α, an EGFR ligand, could not activate the mitogen-activated protein signaling pathway but could partially activate the Akt signaling cascade in PC-9/ZD2001. In PC-9/ZD2001R cells, the association between EGFR and mitogen-activated protein kinase signaling was completely reconstituted. On the basis of this result, we conclude that the decrease of EGFR signaling to the mitogen-activated protein kinase signaling pathway might contribute to acquired gefitinib resistance.[5] In this study, TNF-α significantly induced EGFR autophosphorylation but subsequent activation of the Akt signaling cascade was little observed in PC-9/ZD2001 (Fig. 4A and B). This decreased EGFR signaling on Akt could be partially caused by the decrease in EGFR expression but we have

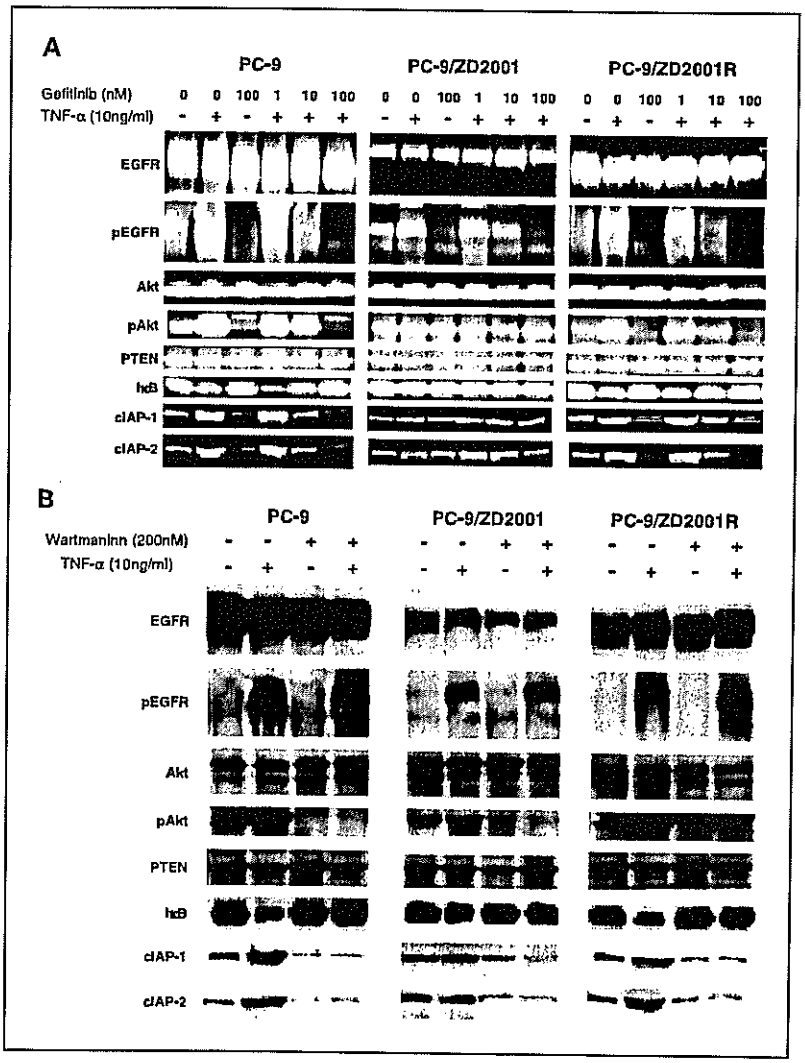

Fig. 4. Inhibitory effect of gefitinib on TNF-α-induced phosphorylation of Akt1 and degradation of IκB. Cells were treated with TNF-α with or without gefitinib (*A*) or wortmannin (*B*) simultaneously for 30 minutes at 37°C. Cell lysates were prepared and equivalent amounts of protein from each cell lysate were resolved with 10% SDS-PAGE, transferred to nitrocellulose membranes, and subjected to Western blotting with specific antibodies (as described in Materials and Methods). The EGFR and Akt1 membranes were stripped and reblotted with antibodies against phospho-EGFR (Tyr1045) and phospho-Akt, respectively. Expression of β-actin was used as internal control. Although treatment with TNF-α significantly phosphorylated EGFR in all three cell lines, downstream Akt/NF-κB activation was observed in PC-9 and PC-9/ZD2001R but weakly in PC-9/ZD2001. Gefitinib inhibited cross-talk signaling in PC-9 and PC-9/ZD2001R cells but not in PC-9/ZD2001 cells (*A*). A phosphatidylinositol 3-kinase inhibitor, wortmannin, completely inhibited this signaling in all three cell lines (*B*).

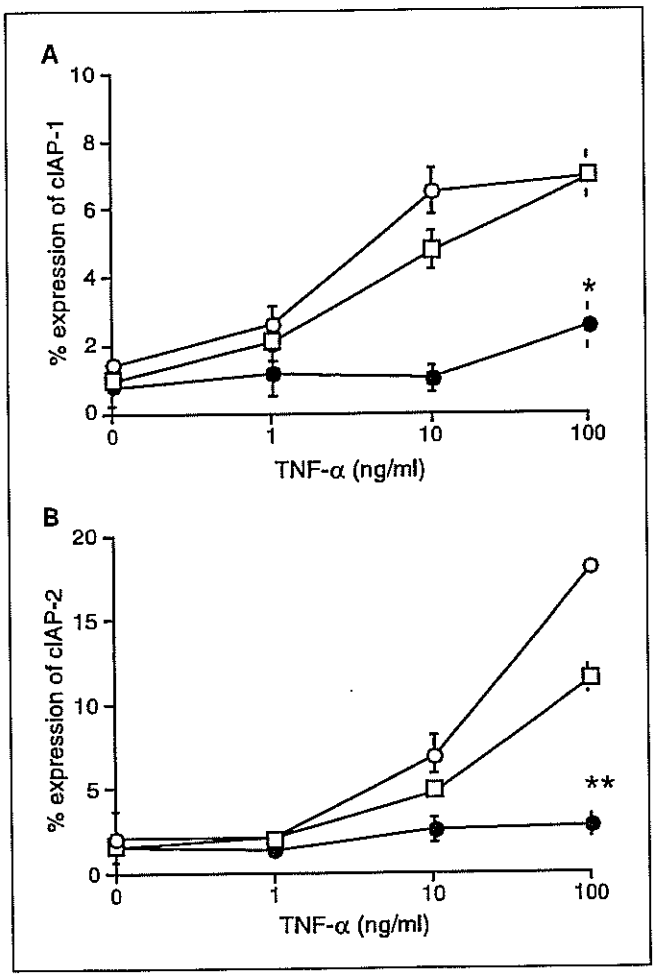

Fig. 5. TNF-α induced c-IAP1 and c-IAP2 mRNA expression in PC-9 and PC-9/ZD2001R cells but not in PC-9/ZD2001 cells. The cells were exposed to the indicated concentrations of TNF-α for 12 hours; after which mRNA was isolated with the guanidium isothiocyanate method. Induction of c-IAP1 (*A*) and c-IAP2 (*B*) mRNA was measured with a fluorescence-based real-time RT-PCR method using specific primer sets (as described in Materials and Methods). The expression levels of c-IAP1 and c-IAP2 mRNA were significantly and dose-dependently increased by exposure to TNF-α in PC-9 and PC-9/ZD2001R cells but this enhancement was rarely observed in PC-9/ZD2001 cells. Results expressed as the percentage of each cell line compared with the internal control, expression of β-actin mRNA. ○, PC-9; ●, PC-9/ZD2001; □, PC-9/ZD2001R. Points, mean of three different experiments; bars, SD. *, $P < 0.001$.

no data to explain the discrepancy between transforming growth factor-α-mediated and TNF-α-mediated EGFR signaling in this cell line. Nevertheless, TNF-α-mediated cross-talk signaling to EGFR, although ligand independent, seems to cause downstream activation in a different way from that caused through ligand-mediated direct EGFR activation. Akt/NF-κB signaling is also known to be downstream of other receptors, such as other Her family receptors (36), platelet-derived growth factor receptor (37), and IFN receptor (38). We previously confirmed the expression of other Her family receptors, Her2 and Her3, in PC-9 cells. Possibly, signaling of these receptors may be able to modulate the TNF-α-mediated cross-talk signaling and Akt/NF-κB signaling. Various aspects of TNF-α-induced cross-talk signaling to EGFR, such as EGFR heterodimer formation with other Her family receptors and downstream signaling specificity, require further investigation.

Human IAPs, c-IAP1 and c-IAP2, have been reported to block the apoptotic events caused by caspase-8 activation by directly combining with caspase-3 and caspase-7 and restraining them (10, 27). IAPs play a key role in the resistance to apoptotic effect of TNF-α superfamily of proteins (39) and various anticancer drugs (40, 41); for this reason, IAPs are considered promising targets in anticancer therapy (42, 43). To evaluate TNF-α-mediated antiapoptotic signaling, we measured IAP induction in these cell lines by means of Western blotting analysis and real-time RT-PCR. As might be expected, IAPs and their mRNAs were markedly induced by TNF-α in PC-9 and PC-9/ZD2001R cells but not in PC-9/ZD2001 cells (Fig. 5A and B). TNF-α-induced activation of caspase-3, but rarely of caspase-8, was significantly lower in PC-9 and PC-9/ZD2001R as compared with PC-9/ZD2001 (Fig. 3A and B). These results suggest that TNF-α precisely activates apoptotic signaling through caspase-8 in all three cell lines and that induction of IAPs blocks downstream signaling by inhibiting caspase-3 in PC-9 and PC-9/ZD2001R. In these cell lines, the induction of IAPs likely plays a key role in determining the sensitivity to TNF-α-mediated apoptosis among the antiapoptotic proteins that are induced by NF-κB-mediated transcription.

Several clinical studies of TNF-α as an anticancer treatment have been done, mainly in the 1970s; however, treatment with TNF-α was greatly limited by its side effects, particularly its toxicity to previously healthy organs (44–49). Recently, several new anticancer therapies using TNF-α have been developed, such as RGD-V29 (F4614) and TNF-erade (Biologic), in an attempt to reduce adverse effects (8, 9, 50, 51). We have shown that a NSCLC cell line with acquired resistance to gefitinib acquired collateral sensitivity to TNF-α. These data strongly suggest that treatment with TNF-α might be effective against tumors that have acquired resistance to gefitinib after long-term administration of this drug. Further analysis is required before clinical application.

In summary, the cross-talk signaling from TNFR to EGFR and subsequent IAP induction play important roles in the resistance to TNF-α-induced apoptosis in PC-9 cells. Because this signaling cascade is decreased in the gefitinib-resistant PC-9/ZD2001 cells, TNF-α did not activate the Akt/NF-κB cascade. This decrease of EGFR signaling to Akt/NF-κB pathway, which is related to gefitinib-acquired resistance, may contribute to the acquisition of hypersensitivity to TNF-α in this cell line.

References

1. Fukuoka M, Yano S, Giaccone G, et al. Multi-institutional randomized phase II trial of gefitinib for previously treated patients with advanced non-small-cell lung cancer (The IDEAL 1 Trial) [corrected]. J Clin Oncol 2003;21:2237–46.
2. Kris MG, Natale RB, Herbst RS, et al. Efficacy of gefitinib, an inhibitor of the epidermal growth factor receptor tyrosine kinase, in symptomatic patients with non-small cell lung cancer: a randomized trial. JAMA 2003;290:2149–58.
3. Kobayashi S, Boggon TJ, Dayaram T, et al. EGFR mutation and resistance of non-small-cell lung cancer to gefitinib. N Engl J Med 2005;352:786–92.
4. Pao W, Miller VA, Politi KA, et al. Acquired resistance of lung adenocarcinomas to gefitinib or erlotinib is associated with a second mutation in the EGFR kinase domain. PLoS Med 2005;2:e73.
5. Ashkenazi A. Targeting death and decoy receptors of the tumour-necrosis factor superfamily. Nat Rev Cancer 2002;2:420–30.
6. Basile JR, Zacny V, Munger K. The cytokines tumor